Spin Transfer Torque Point Contacts

W. Van Roy

IMEC, Kapeldreef 75, B-3001 Leuven, Belgium

vanroy@imec.be

Maarten van Kampen
Sven Cornelissen
Xavier Janssen
Mauricio Manfrini
Liesbet Lagae

Quentin Mistral
Joo-Von Kim
Thibaut Devolder
Paul Crozat
Claude Chappert

Gino Hrkac
Thomas Schrefl

Helmut Schultheiss
B. Obry
S. Hernsdörfer
A. Laraoui
Burkard Hillebrands

FP6-RTN SPINSWITCH

FP6-IST TUNAMOS

Outline

- **Spin torque & applications**
  - MRAM, racetrack memory, spin torque oscillator (STO)
  - Noise source in HD read heads
- **Point contacts : vortex oscillations**
- **Point contacts : spin wave generation**
- **Dynamics in magnetic semiconductors**

Spintronics ?

- Key technology behind **magnetic data storage**
  - Ultra-sensitive read heads drive Moore's law in HD data storage
- Many other (potential) applications
  - **Sensors: biosensors, automotive, positioning, …**
  - MRAM
  - Spin-torque oscillators
  - **"Dirty" environments** (radiation hardness, …)

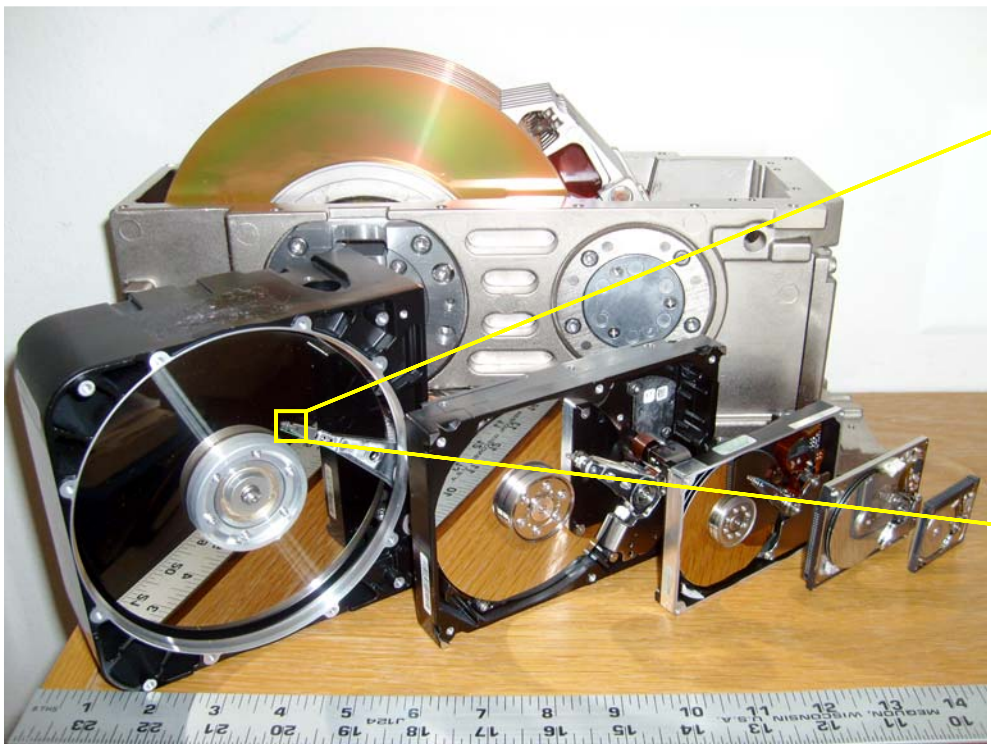

MRAM

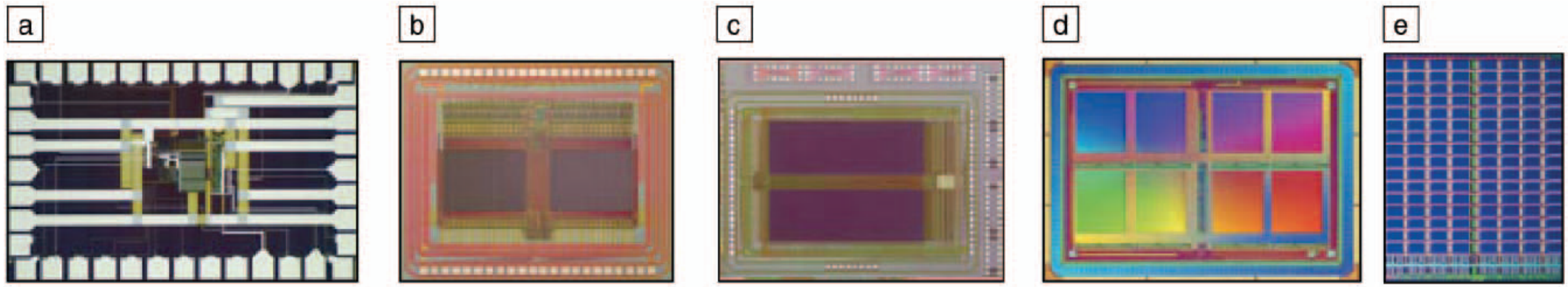

Figure 2. Photomicrographs showing the increasing density of prototype magnetic random-access memory (MRAM) chips. (a) IBM 1 mm × 1.5 mm, 1 kbit chip with a 5.4-μm^2 twin cell in 0.25-μm technology with approximately 3–10-ns access time (from Reference 22, with permission). (b) Motorola 3.9 mm × 3.2 mm, 256 kbit chip with 7.1-μm^2 cell in 0.6-μm technology with 50-ns access time (from Reference 23, with permission). (c) Motorola 4.25 mm × 5.89 mm, 1 Mbit chip with 7.1-μm^2 cell in 0.6-μm technology with 50-ns access time (from Reference 24, with permission). (d) Motorola 4.5 mm × 6.3 mm, 4 Mbit chip with 1.55-μm^2 cell in 180-nm technology with 25-ns access time (from Reference 17, with permission). (e) IBM 7.9 mm × 10 mm, 16 Mbit chip with 1.42-μm^2 cell in 180-nm technology with 30-ns access time (adapted from Reference 21, with permission).

S. Wolf, MRS Bulletin (May 2006)

- **Cross-point**
  - Failed
- **Toggle MRAM**
  - Up to ~2006: steady increase in size of demonstrators
  - Only 1 product (Motorola / Freescale / Everspin): scaling issues
- **Spin torque MRAM**
  - Scaling much better
  - Industry side: is picking up momentum after a few years of silence

Domain wall motion based: Racetrack memory

S. Parkin (IBM), Patent US 6,955,926 B2 (2005)

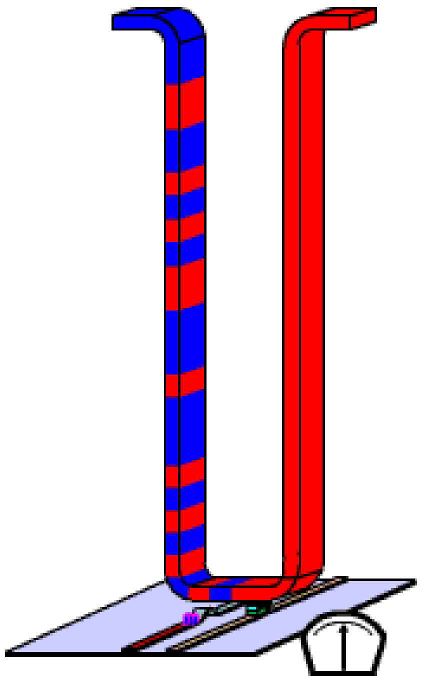

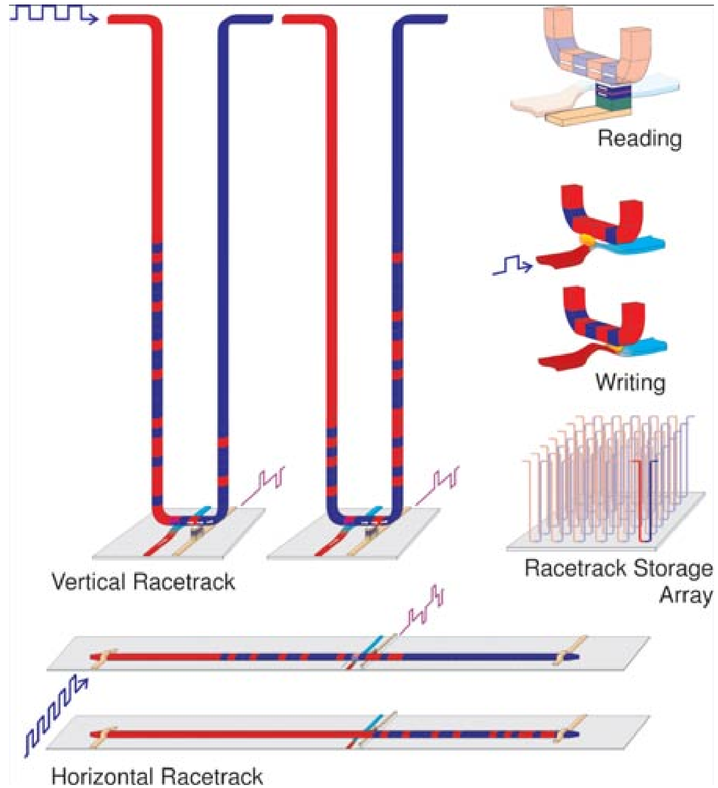

- Session II (Thursday): **Nanowires & Domain Wall Propagation**

Low-cost tunable radio on a Si chip

NEEDED: -15 dBm (3uW) output power

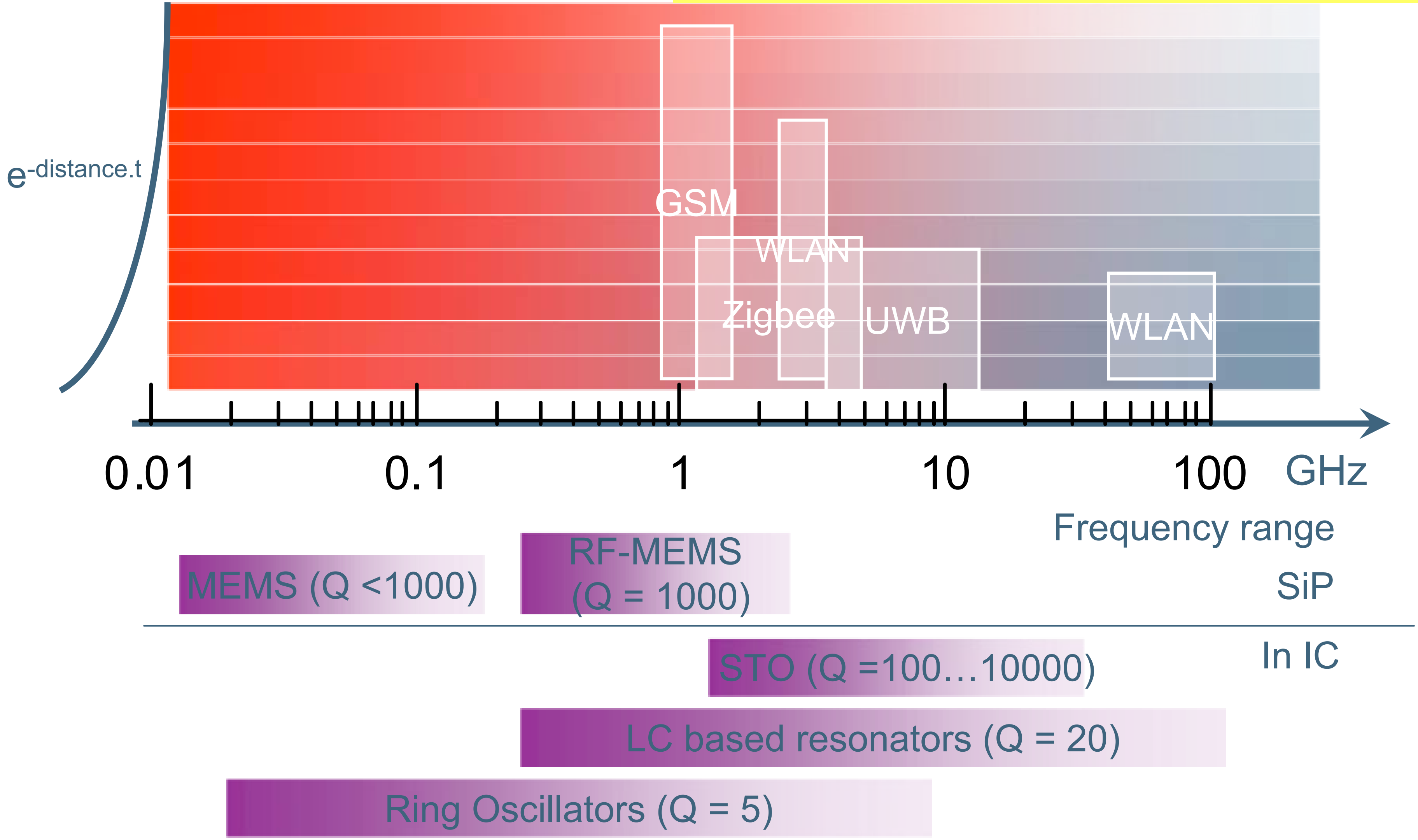

Competition: LC based VCO above IC

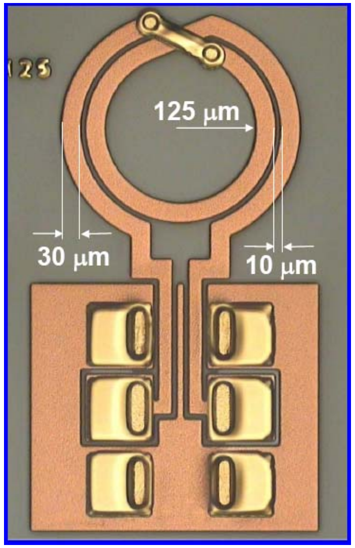

High quality coil
- Thick Cu
- High k dielectric

5 GHz VCO
On 90 nm

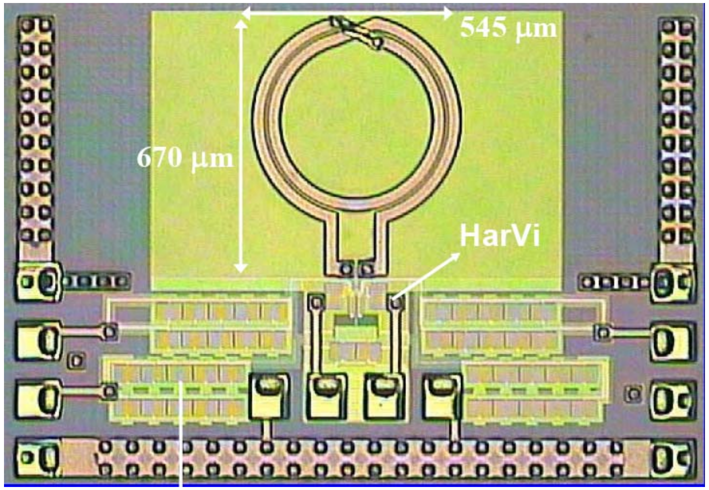

UWB VCO
on 0.35 um

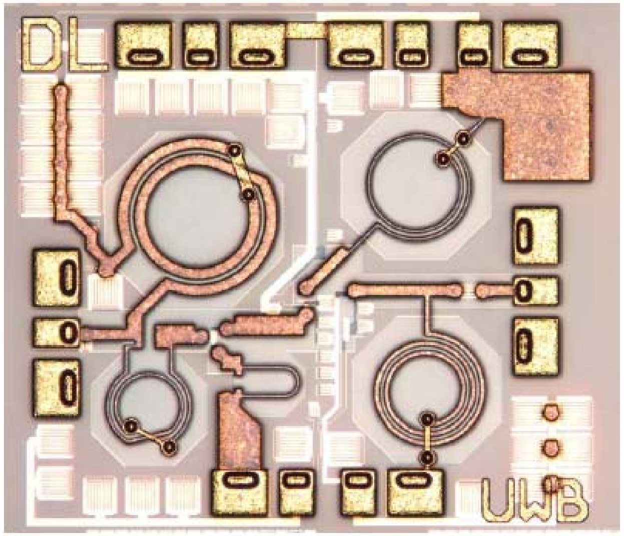

Competition: RF-MEMS

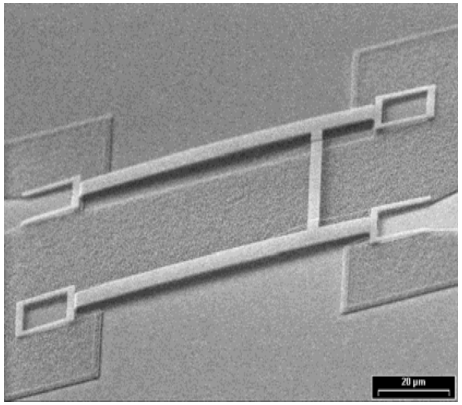

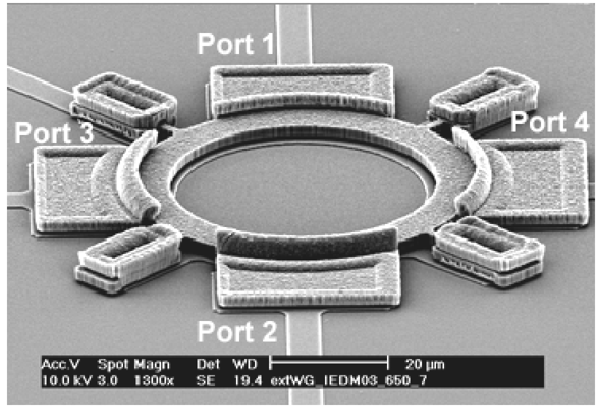

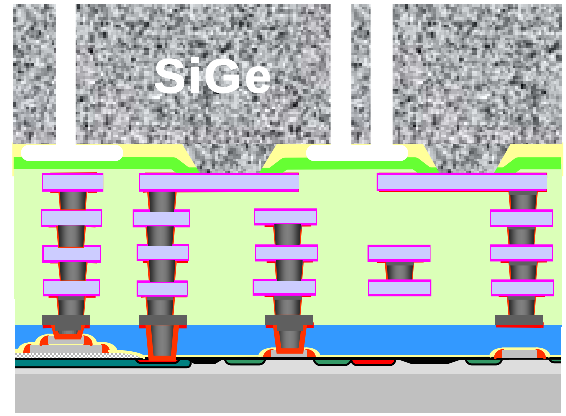

RF MEMS Resonators in Poly SiGe (IMEC)

- Lower processing temperature (400C) compared to poly-Si on top of IC possible !!!
- Electromechanical properties very similar to poly-Si High quality factors (3000)

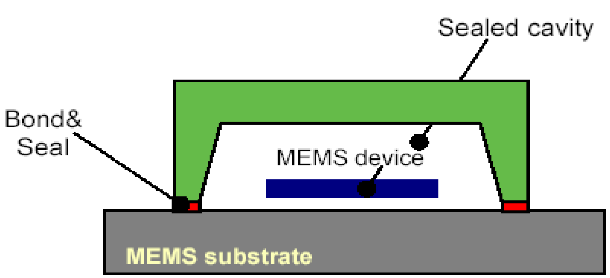

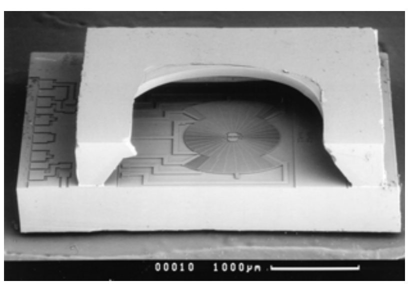

Vacuum package

Compared to existing oscillator technologies

f = 5 - 10 GHz	VCO- LC 	VCO- L high K 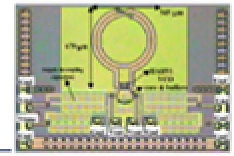	RF MEMS 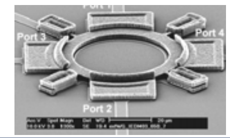	VCO- STO 
Size	500 um^2	1 mm^2	1 mm^2	1 um^2
Q	18 (classical on chip inductor)	100 (enhanced inductor)	1000	> 1000
Output power/	- 10 dBm	0 dBm	0 dBm	>- 15 dBm
Phase noise and long term stability	-117 dBc @ 400 kHz	-115 dBc	-110 dBc	< -110 dBc?
Power consumption	8 mA @ 2.5V	0.4 mA @ 0.82 V	35 mA @ 3.3V	1-5 mA @ 1V
Tunable range	20 %	10 %	1 %	**10-100%**
Agility	microseconds	microseconds		Nanoseconds

Spintronics ?

- Key technology behind **magnetic data storage**
  - Ultra-sensitive read heads drive Moore’s law in HD data storage
- Many other applications
  - Sensors (biosensors, automotive, …)
  - MRAM
  - Spin-torque oscillators
  - “Dirty” environments (radiation hardness, …)

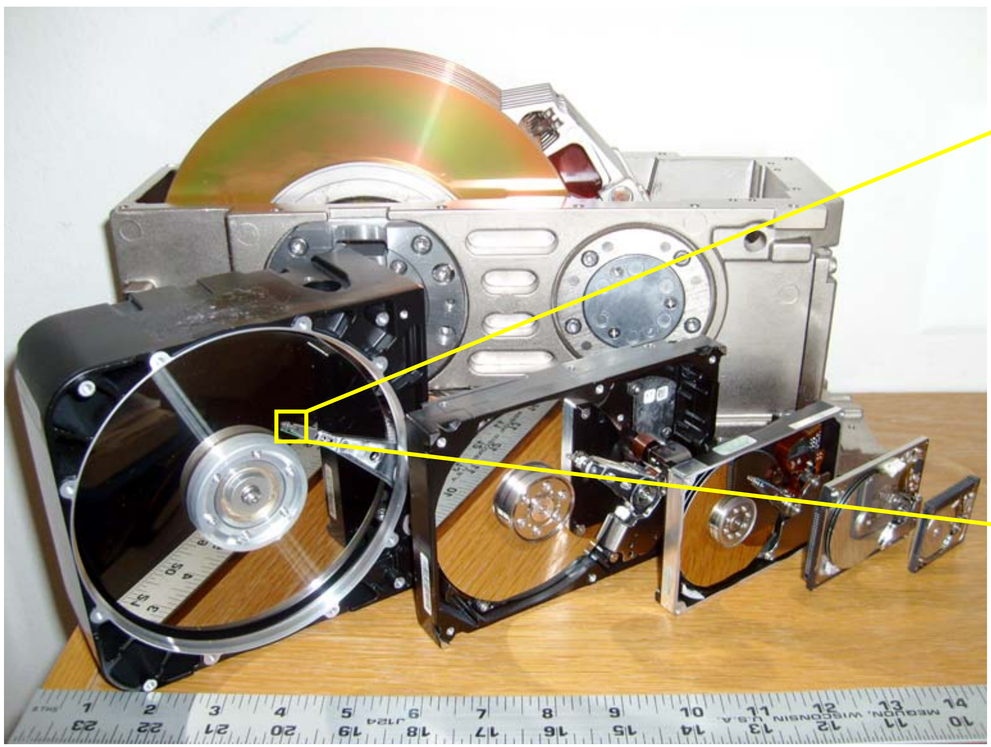

Noise in GMR sensors: thermally excited FMR

J. C. Jury, ***"Measurement and Analysis of Noise Sources in GMR Sensors Up to 6 GHz,"*** IEEE Trans. Magn. **38**, 3545 (2002). (Stanford & IBM)

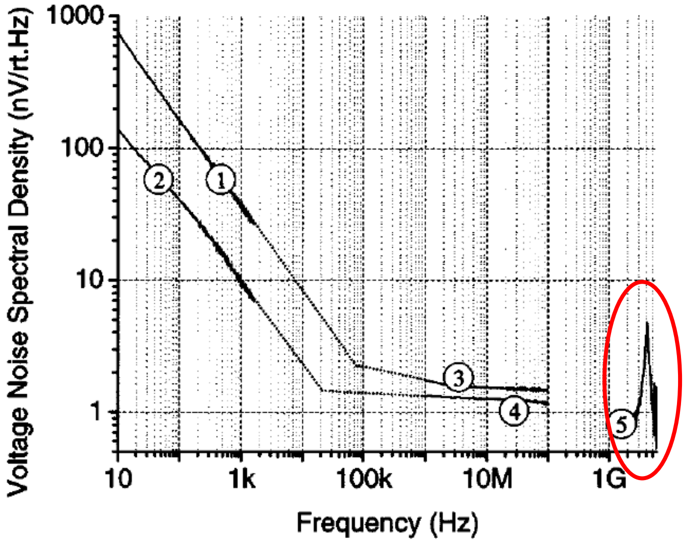

Fig. 1. Voltage noise spectral density for a typical GMR sensor (nonsaturated and saturated). Solid traces indicate actual measured data. Traces 1 (nonsaturated) and 2 (saturated) indicate $1/f$ noise. Traces 3 (nonsaturated) and 4 (saturated) indicate thermal (electrical and magnetic) fluctuation noise. Dotted lines extrapolate these traces to their intercept points. Trace 5 indicates the resonance in the magnetic fluctuation noise (at about 5 GHz).

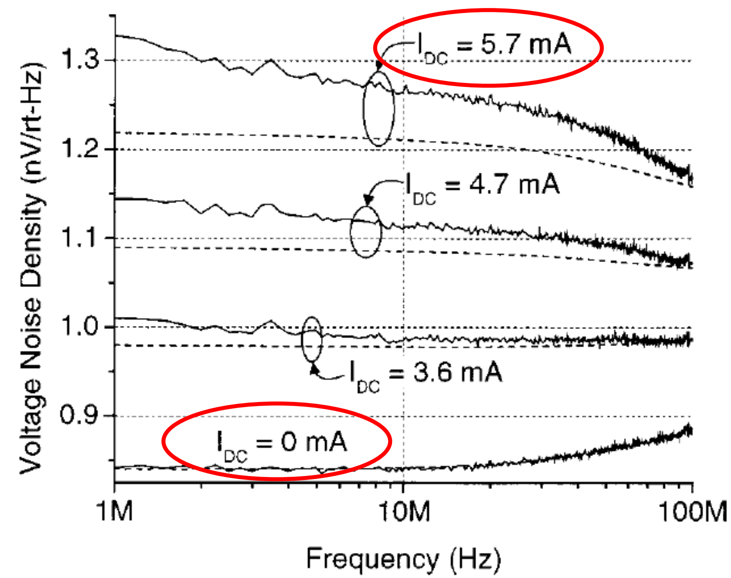

Fig. 5. Measured voltage noise density for saturated type B sensors at various bias currents. Solid line: measured noise at specified bias current. Dashed line: expected noise from measured ac resistance.

Also: Y. Zhou, *"Experimental observations of thermally excited ferromagnetic resonance and mag-noise spectra in spin valve heads,"* MMM-46 (Seattle, 2001), Paper CB-06.

Noise in GMR sensors: ... and more

J.-G. Zhu, ***"Current Induced Noise in CPP Spin Valves,"*** IEEE Trans. Magn. **40**, 2323 (2004). (Carnegie Mellon & Headway Technologies)

I. INTRODUCTION

CURRENT perpendicular-to-plane (CPP) read head designs, such as magnetic tunnel junction (MTJ), spin-valve [1], and giant magnetoresistive (GMR) multilayer [2] designs can potentially provide high readback amplitude at deep submicrometer track widths. CPP spin valves are of particular interest because they have low Johnson noise and are shot noise free, in comparison with MTJ read heads.

in a CPP spin-valve head, the spin transfer effect can induce a substantial magnetic noise with a pronounced $1/f$ spectral content if a critical current density is exceeded

Noise in GMR sensors: ... and more

J.-G. Zhu, ***"Current Induced Noise in CPP Spin Valves,"*** IEEE Trans. Magn. **40**, 2323 (2004). (Carnegie Mellon & Headway Technologies)

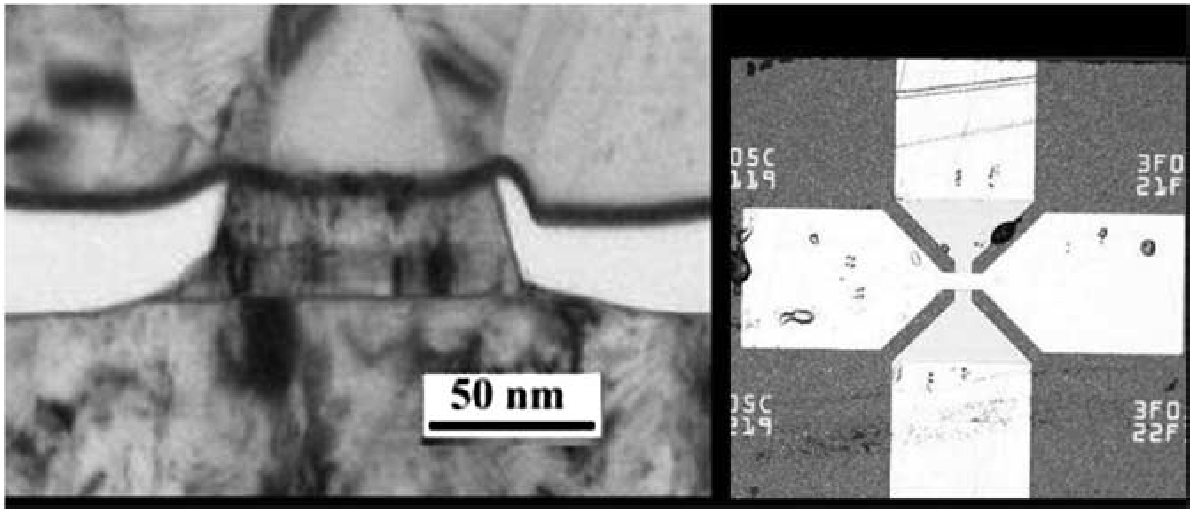

Fig. 1. Cross-section transmission electron micrograph of the CPP read sensor stack, patterned into a 95×95 nm^2 square at the free layer level (left) and the contacting pads.

Noise in GMR sensors: SMT noise

J.-G. Zhu, ***"Current Induced Noise in CPP Spin Valves,"*** IEEE Trans. Magn. **40**, 2323 (2004). (Carnegie Mellon & Headway Technologies)

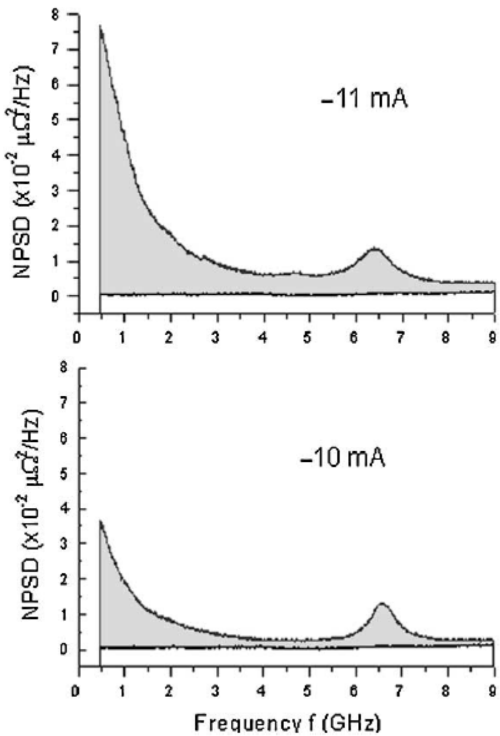

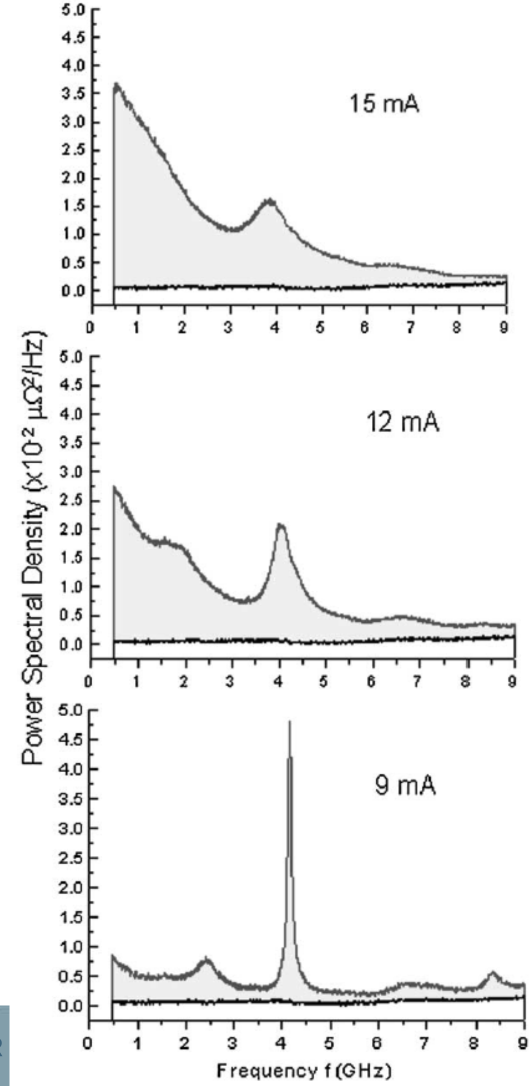

Noise in GMR sensors: SMT noise

J.-G. Zhu, ***"Current Induced Noise in CPP Spin Valves,"*** IEEE Trans. Magn. **40**, 2323 (2004). (Carnegie Mellon & Headway Technologies)

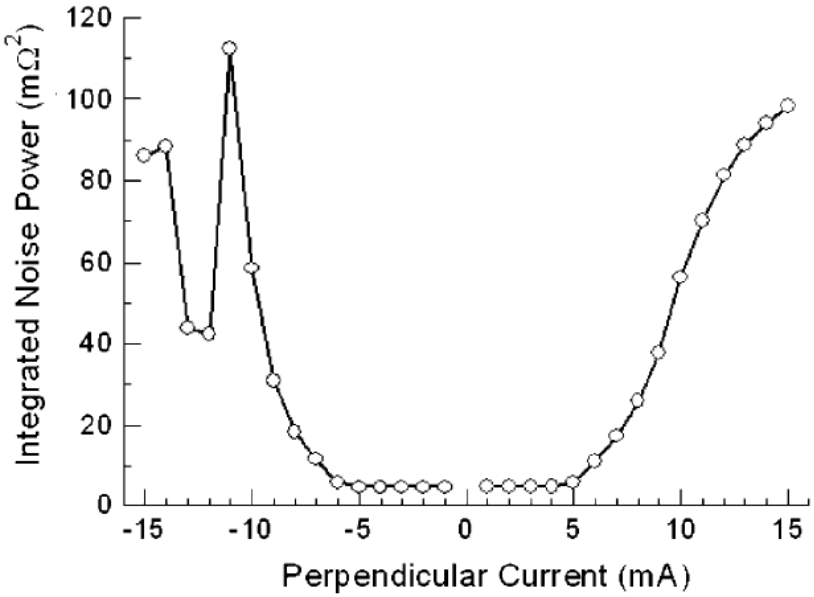

Fig. 5. Integrated resistance noise power as a function of sense current, measured in zero magnetic field. Noise criticality in either current direction is evident.

Also: M. Covington, "***Current-induced magnetization dynamics in current perpendicular to the plane spin valves,***" PRB **69**, 184406 (2004). (Seagate)

Vortex oscillations in nanopoint contacts

- Fabrication: IMEC
- Characterization: IEF-UPS, IMEC
- Modelling: U.Sheffield, IEF-UPS

Precession:
the fast dynamics of the magnetization

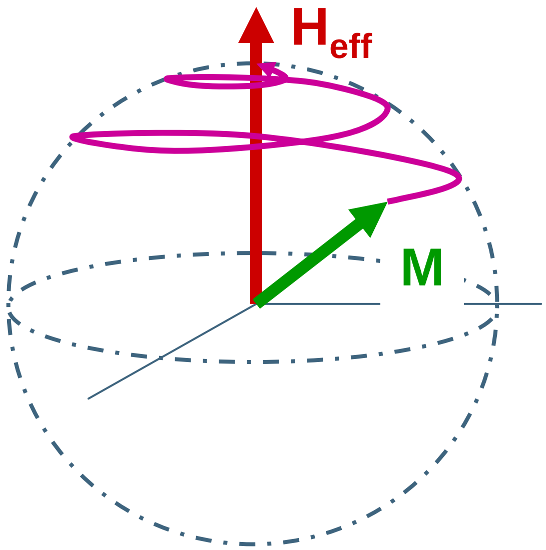

Damped precession **of the magnetization M around its equilibrium axis**

Effective field H_{eff} : **all magnetic energies of the system**

Precession frequency: $f = f_0 H_{eff}$

f_0 = 28 MHz / mT (= 2.8 GHz / kOe)

natural precession frequencies in the 1–10 GHz range with usual 3d ferromagnetic metals
➔ can we overcome damping for applications ?

Spin-torque oscillators

Technical realizations:

„Nano-Pillar“

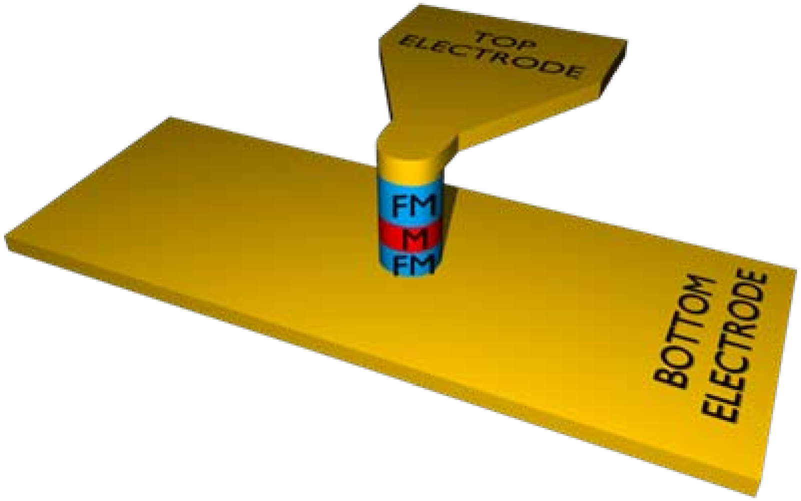

„Nano-Contact“

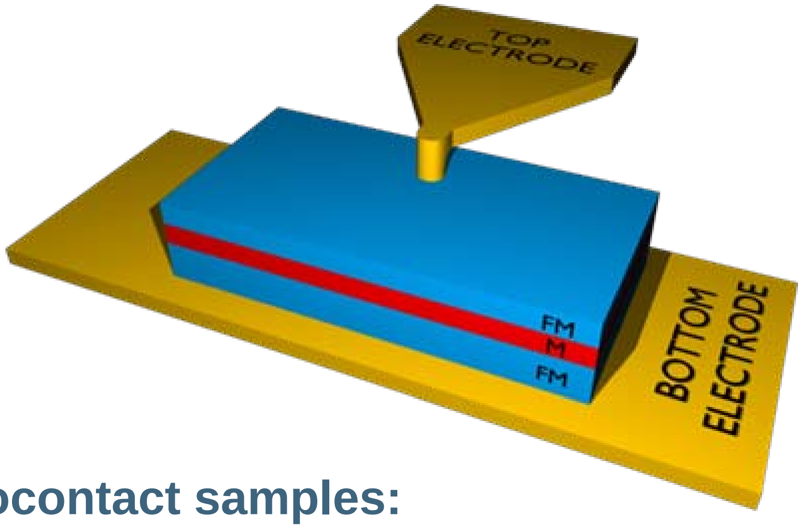

Nanocontact samples:

- In-plane radius of active area: ≈ 20 - 200 nm
- „Free“ layer thickness: 2 - 5 nm
- „Fixed“ layer thickness: 10 - 20 nm
  (pinned with antiferromagnet)
- Current density: ≈ 10^8 - 10^9 A/cm^2

RF emission from nano-contacts

Point contact geometry

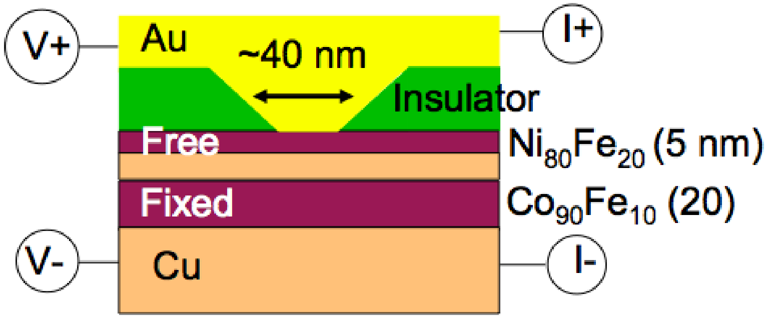

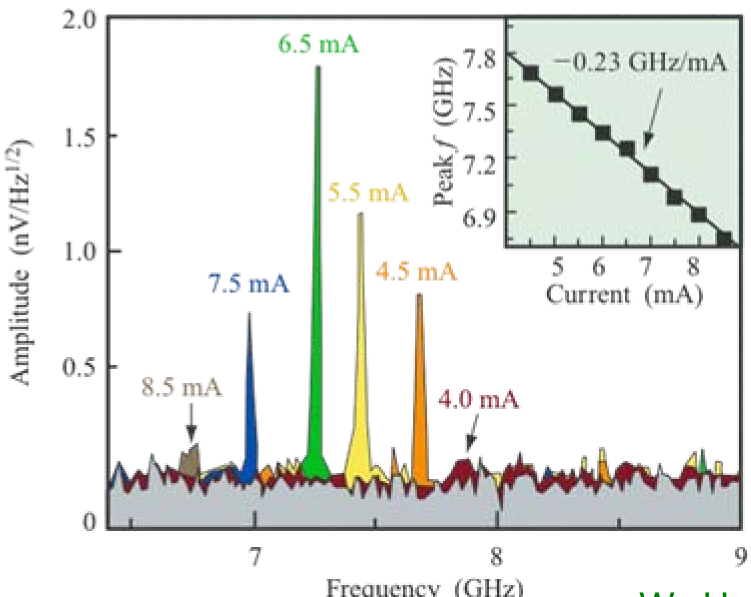

Parametric excitation of spin waves due to spin-momentum transfer

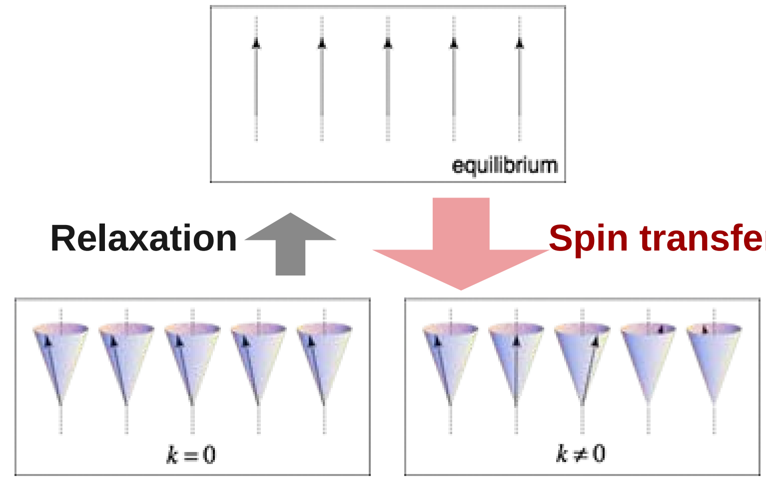

Microwave emission

Frequency tunable with field and current

Q > 10 000

W. H. Rippard et al., Phys. Rev. Lett. 92, 027201 (2004)

RF emission from nano-contacts

a reference measurement

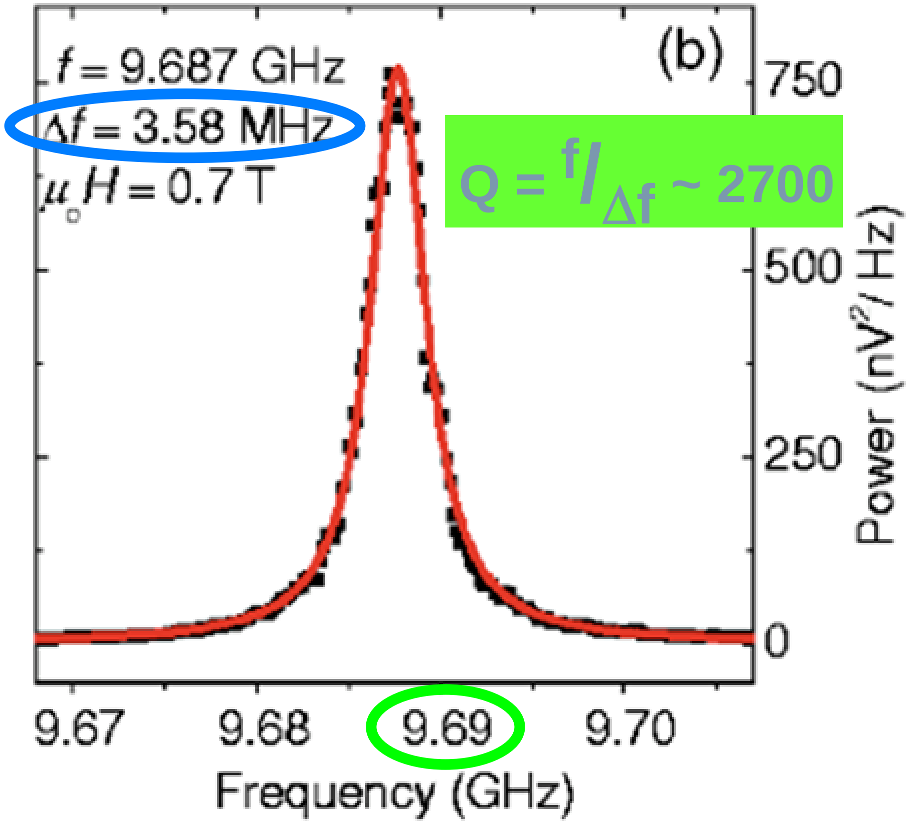

$Q = {}^{f}/_{\Delta f} \sim 2700$

- spin valve stack with $\Delta R = 140 m\Omega$
- applied field $\mu_0 H = 0.7$ T

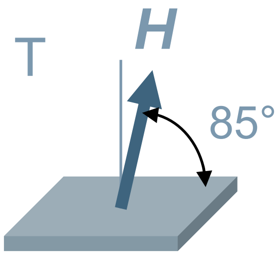

- output voltage: 93 μV (on 50Ω load)

in different conditions:
lower power
but record Q ~18100

W. H. Rippard et al., Phys. Rev. B 70, 100406 (2004)

Point-contact fabrication

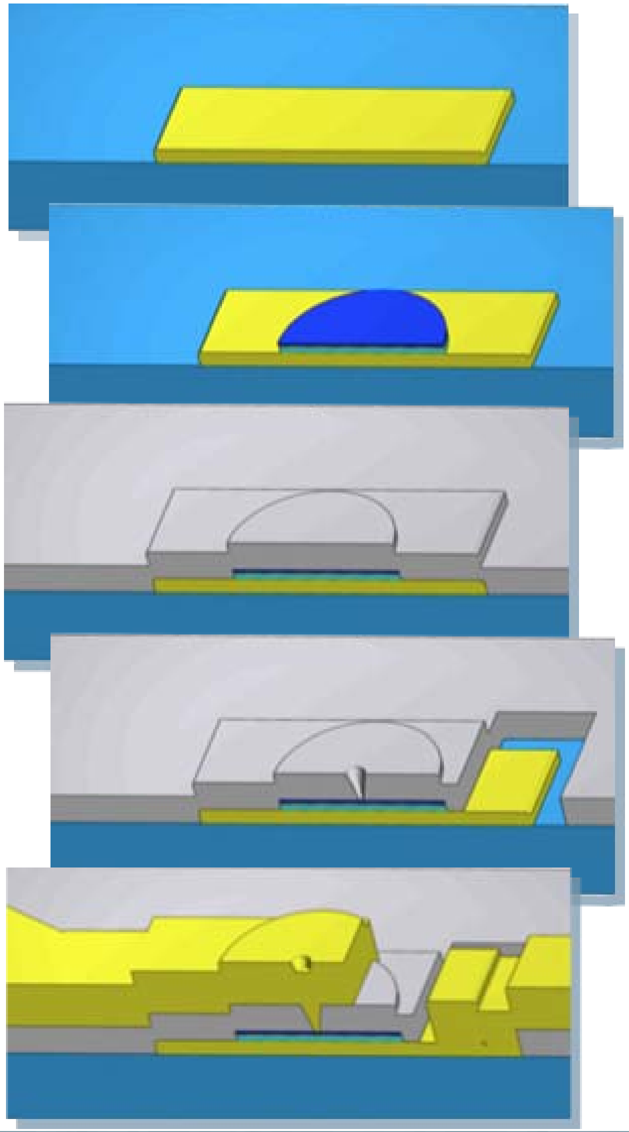

1. Cu bottom electrode
2. Spin valve deposition and ion milling (17 x 27 µm)
3. Passivation with SiO_2
4. E-beam lithography and *wet etching* of point contact and vias
5. Top contact definition using metal (Au) lift-off

Point contact morphology

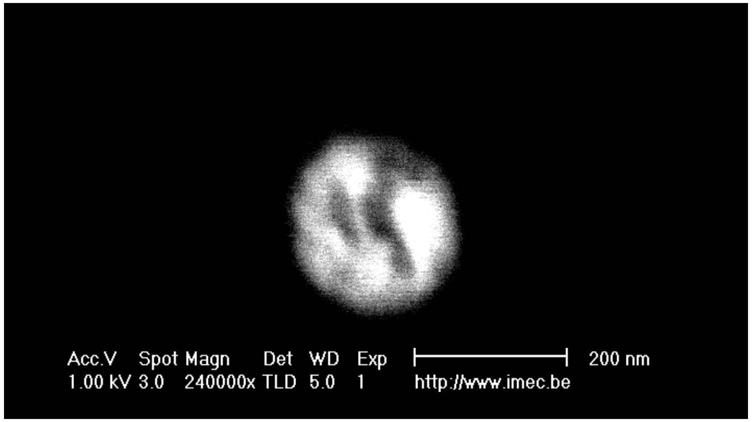

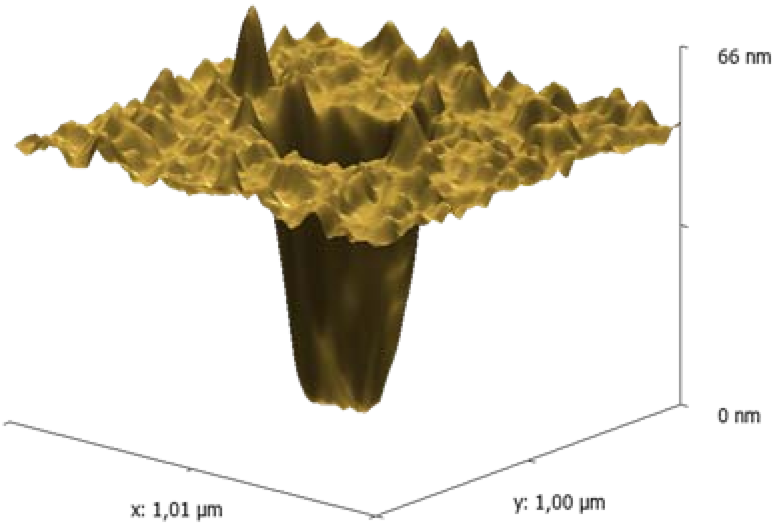

Point contact morphology

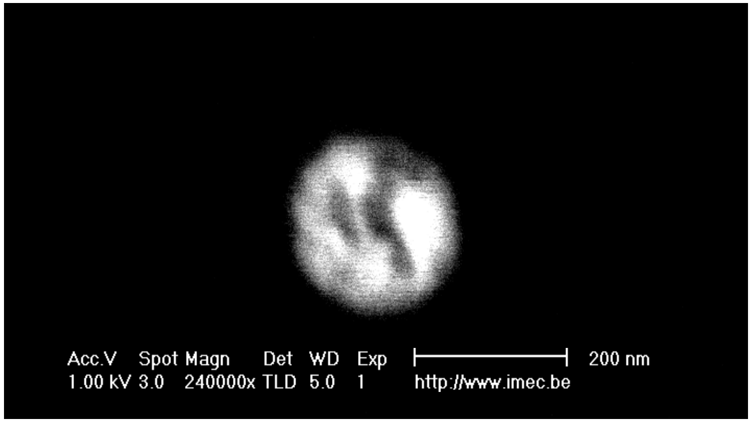

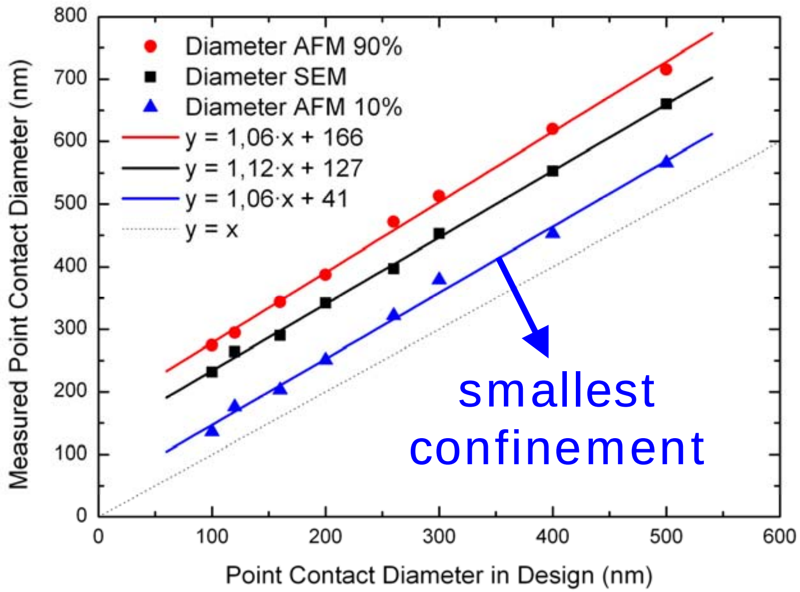

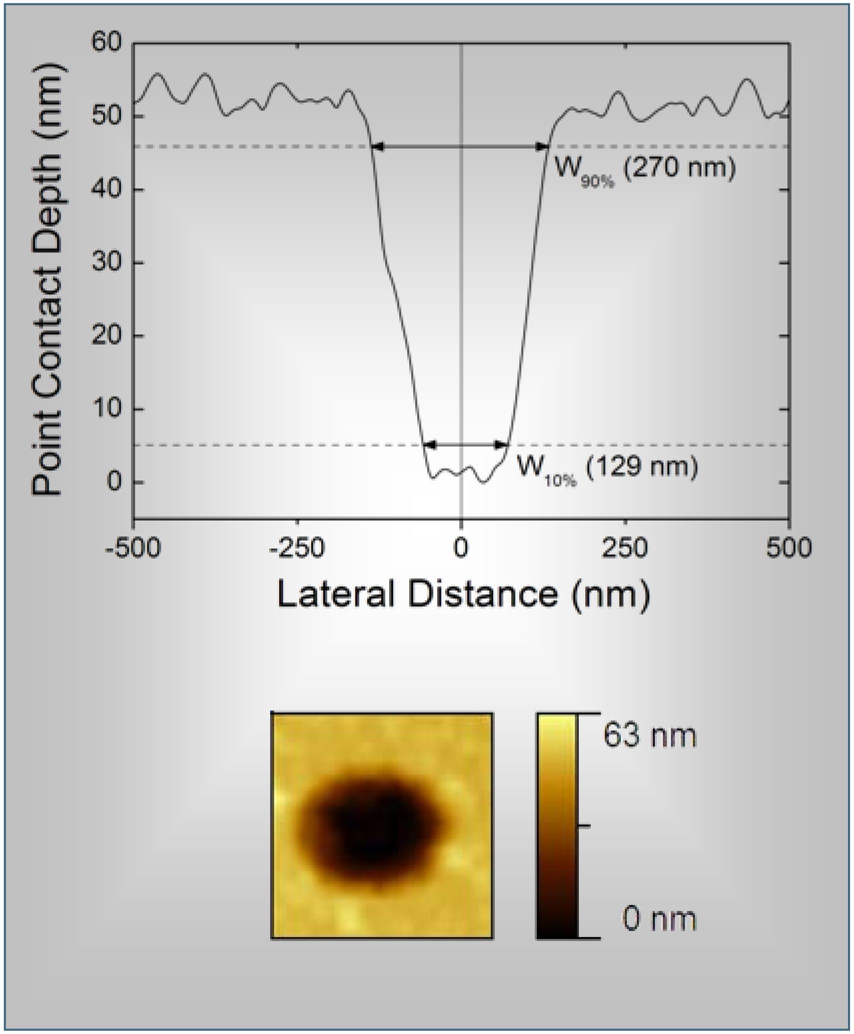

Magnetic and MR properties

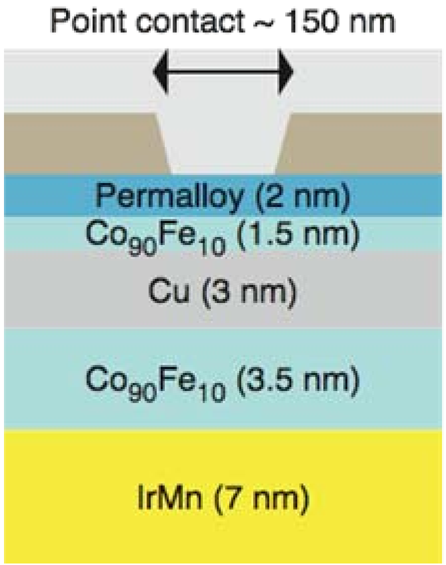

Free layer

$$\left\{ \begin{array}{l} \mu_0 M_s = 1.1\,\mathrm{T} \\ \mu_0 H_k = 1.4\,\mathrm{mT} \end{array} \right.$$

Pinned layer

Spin-valve stack

$$\Delta R \sim 20\,\mathrm{m}\Omega$$

CPP-GMR

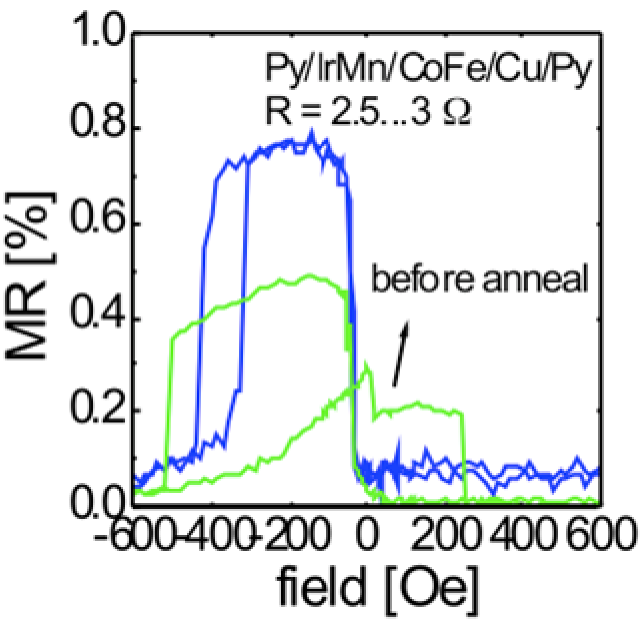

RF measurements

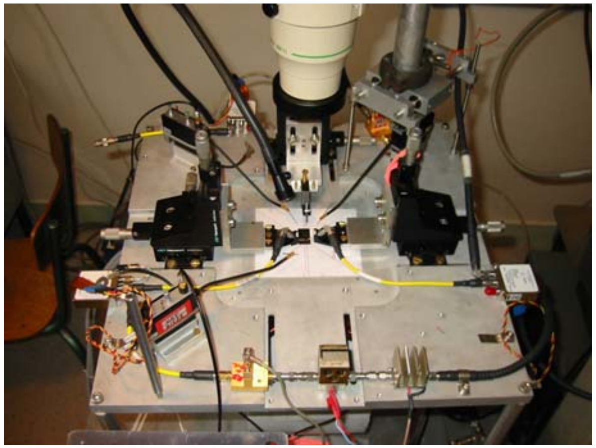

- Variable < 3.5 kOe in-plane and perp-to-plane fields
- Permanent magnets (~ 5 kOe) for large perp. fields

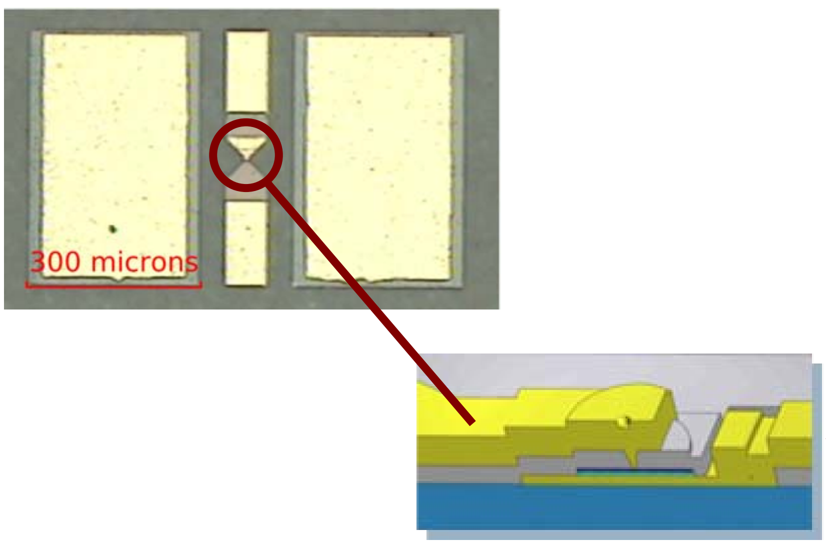

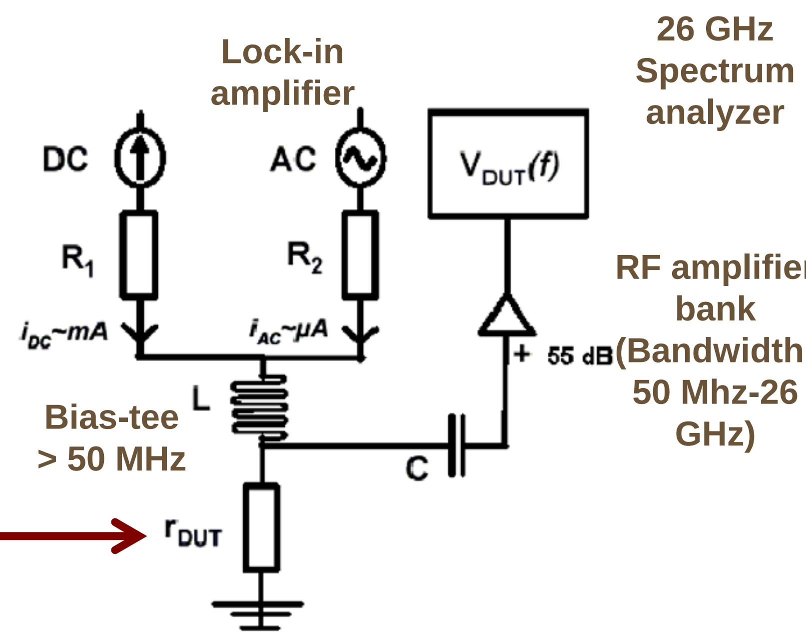

Low frequency power spectra

Mistral, van Kampen et al., PRL **100**, 257201 (2008)

- Perpendicular applied fields

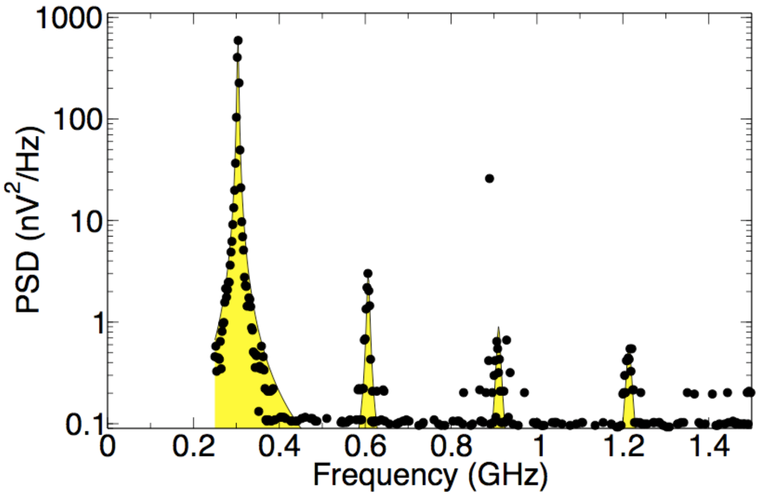

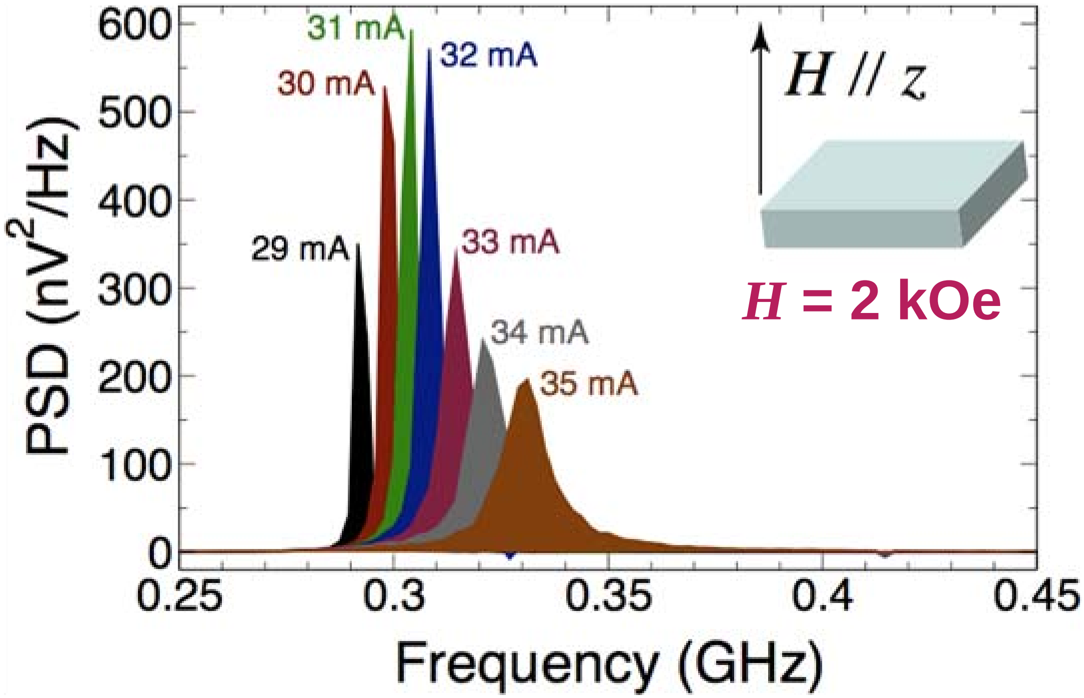

- Largely circular magnetization precession
- **Δf = 1.2 MHz @ f_0 = 299 MHz**

Vortex oscillations in magnetic dots

Field-driven

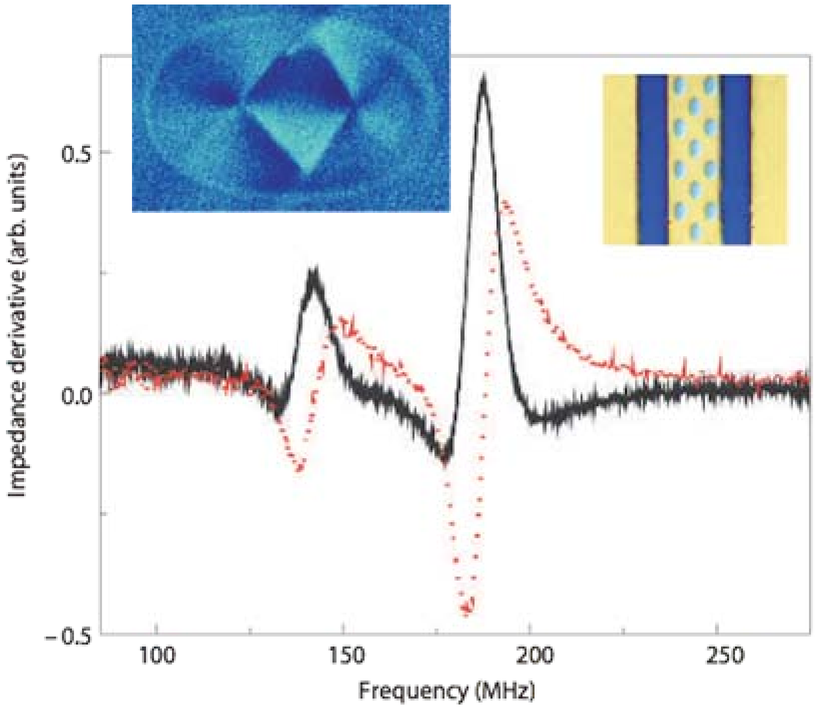

K. S. Buchanan, Nat. Phys. **1**, 172 (2005)

Current-driven

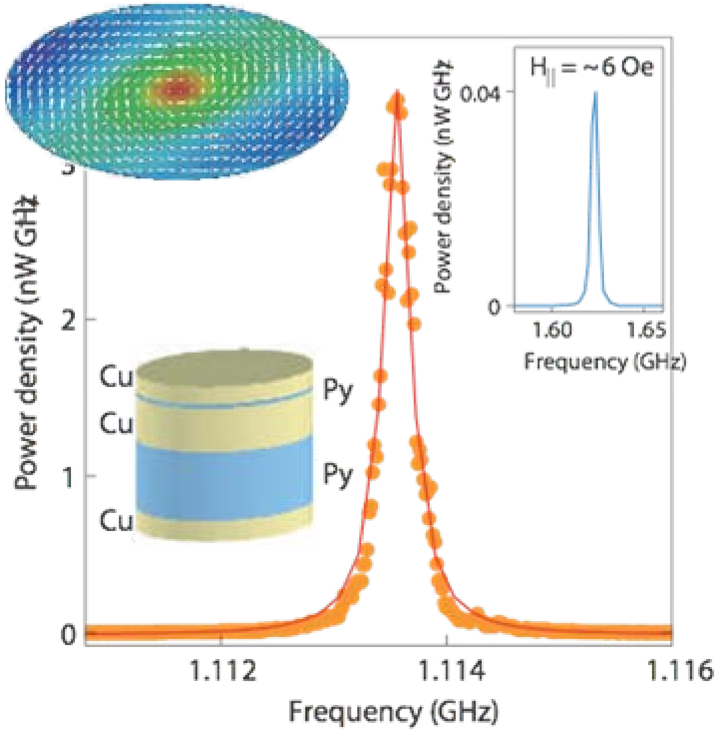

V. Pribiag et al., Nat. Phys. **3**, 498 (2007)

Geometry: Confining potential

Vortex oscillations in point contacts?

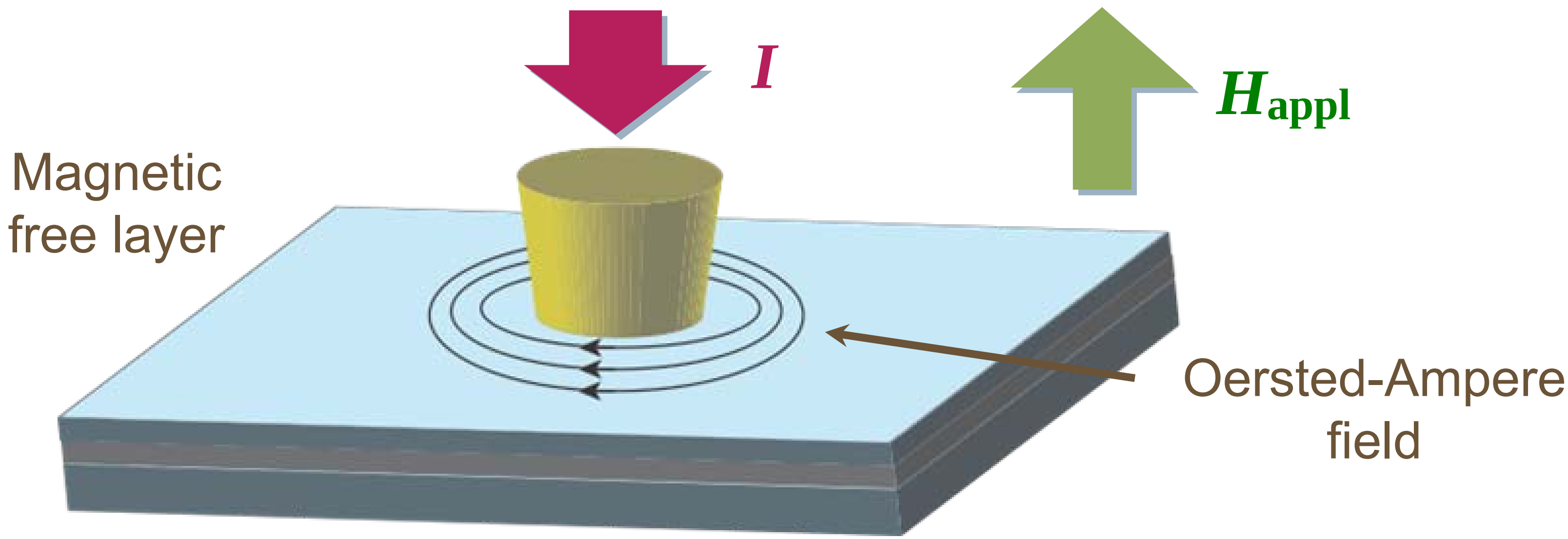

Oersted field as confining potential?

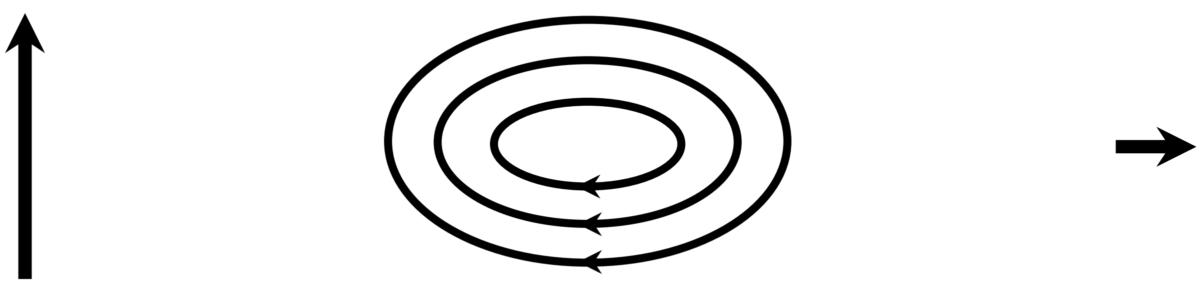

$\mu_0 H_0$ **~ 0.5 T** $\mu_0 H_{Oe}$ **~ 0.06 T @ 30 mA** $\mu_0 H_k$ **~ 0.001 T**

Low frequency power spectra

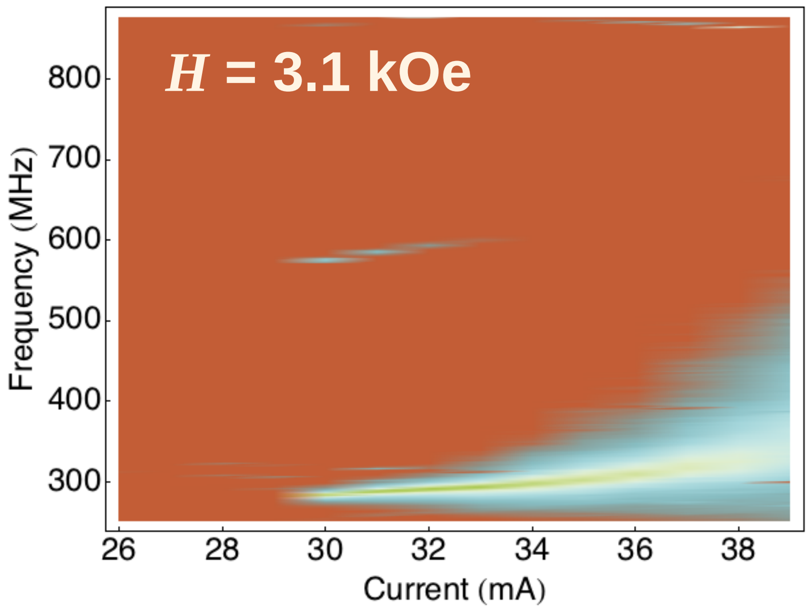

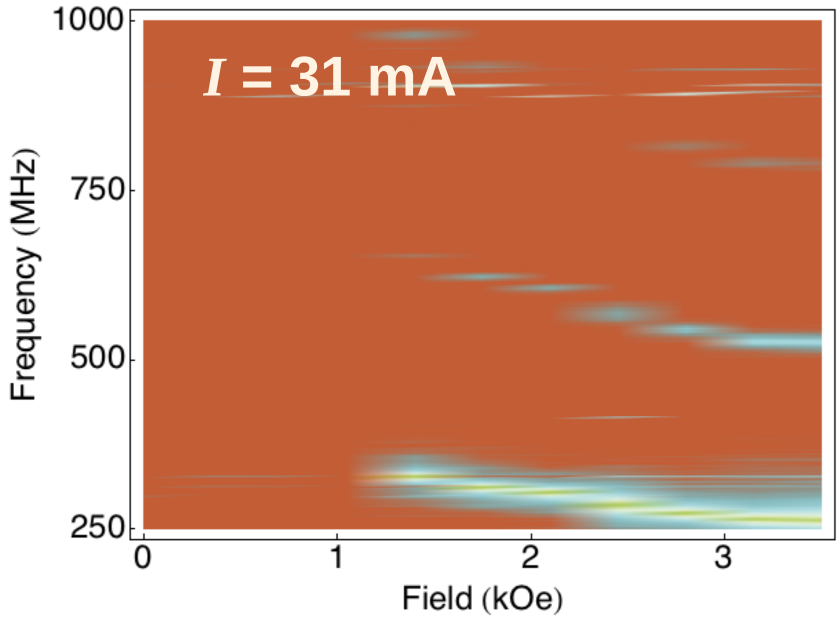

- Quasi-linear variation with current
- f_0 : 250-400 MHz

- “Threshold” field for oscillations
- If FMR: $f_0 \sim 1$ GHz

Zero-field oscillations

I **= 28 mA**

- Oscillations "nucleated" at high fields persist to **zero** applied field

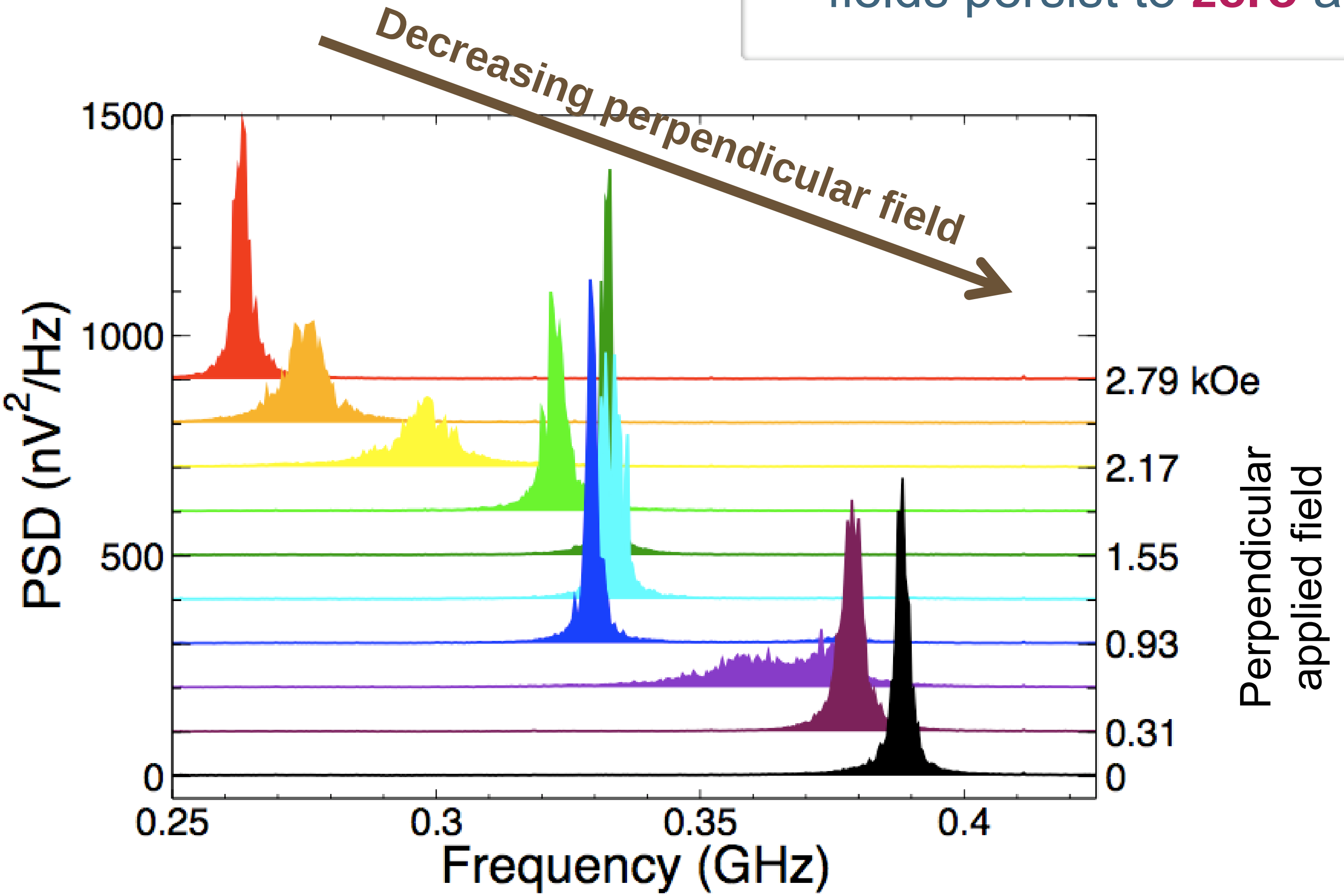

(In-)Sensitivity to in-plane fields

***I* = 28 mA**

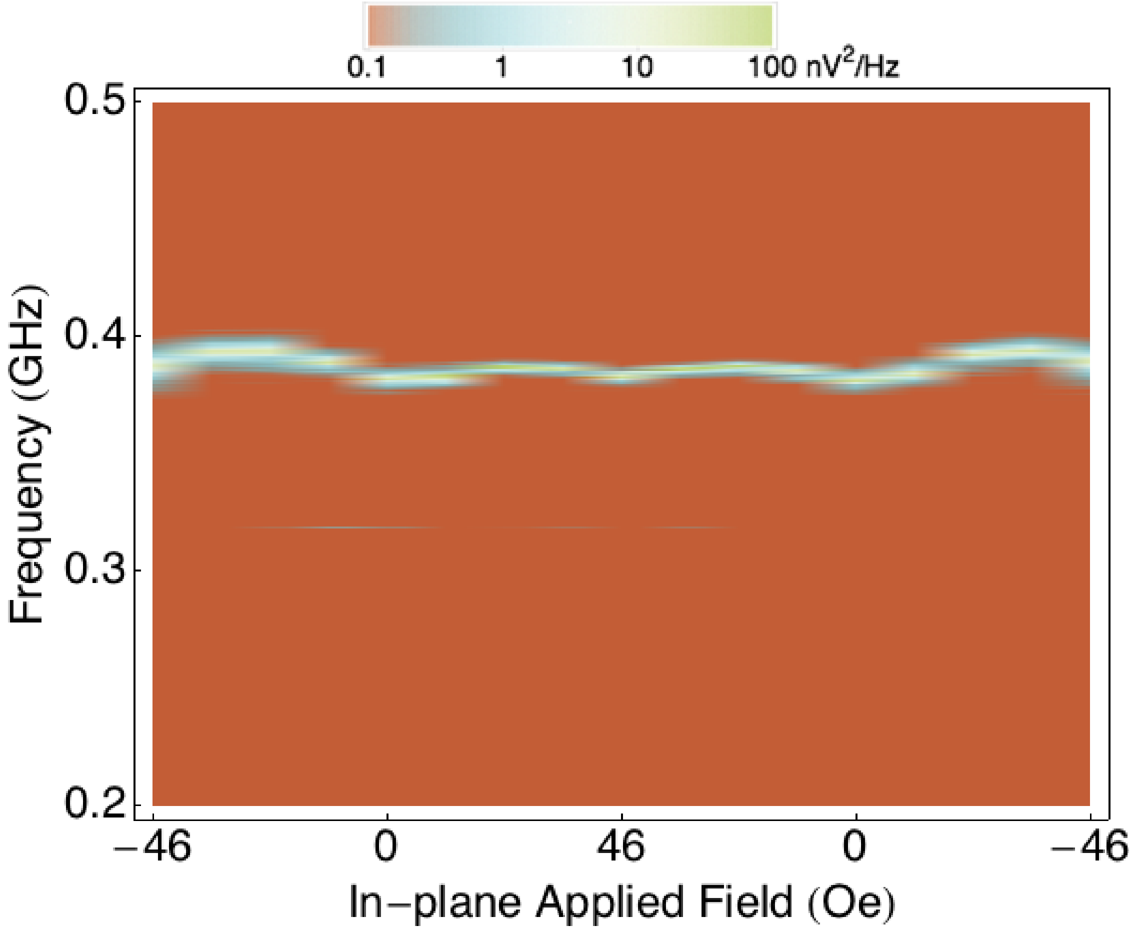

In-plane field sweep

- Start with zero-field oscillation
- Sweep field in film plane
- Best peak = dipolar field bias (Néel coupling) compensated
- stable up to 150-200 Oe
- completely suppressed above

Micromagnetics simulations

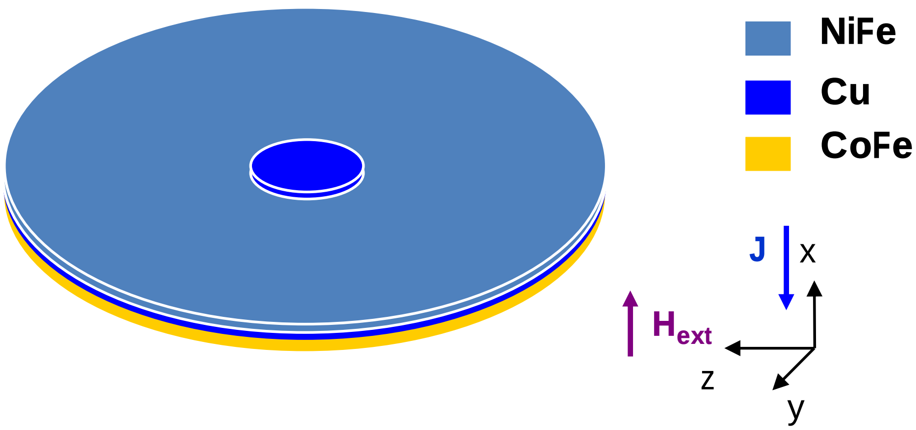

Point contact radius 80 nm

Simulation area radius - 1 μm

LLG + Slonczewski

$$\frac{\partial \mathbf{m}}{\partial t} = -\frac{\gamma}{1+\alpha^2}\mathbf{m}\times\mathbf{h} - \alpha\frac{\gamma}{1+\alpha^2}\mathbf{m}\times(\mathbf{m}\times\mathbf{h}) + \beta\frac{1}{1+c_p\mathbf{m}\cdot\mathbf{e}_p}\left[\mathbf{m}\times(\mathbf{m}\times\mathbf{e}_p)\right]$$

$\mathbf{h} = \mathbf{h}_{exchange} + \mathbf{h}_{anis} + \mathbf{h}_{demag} + \mathbf{h}_{ext} + \mathbf{h}_{oersted}$

+ inhom. **J** distribution (nanocontact exact profile)

Micromagnetics simulations

Mistral, van Kampen, Hrkac et al., PRL **100**, 257201 (2008)

Simulations show vortex orbits *outside* point contact region

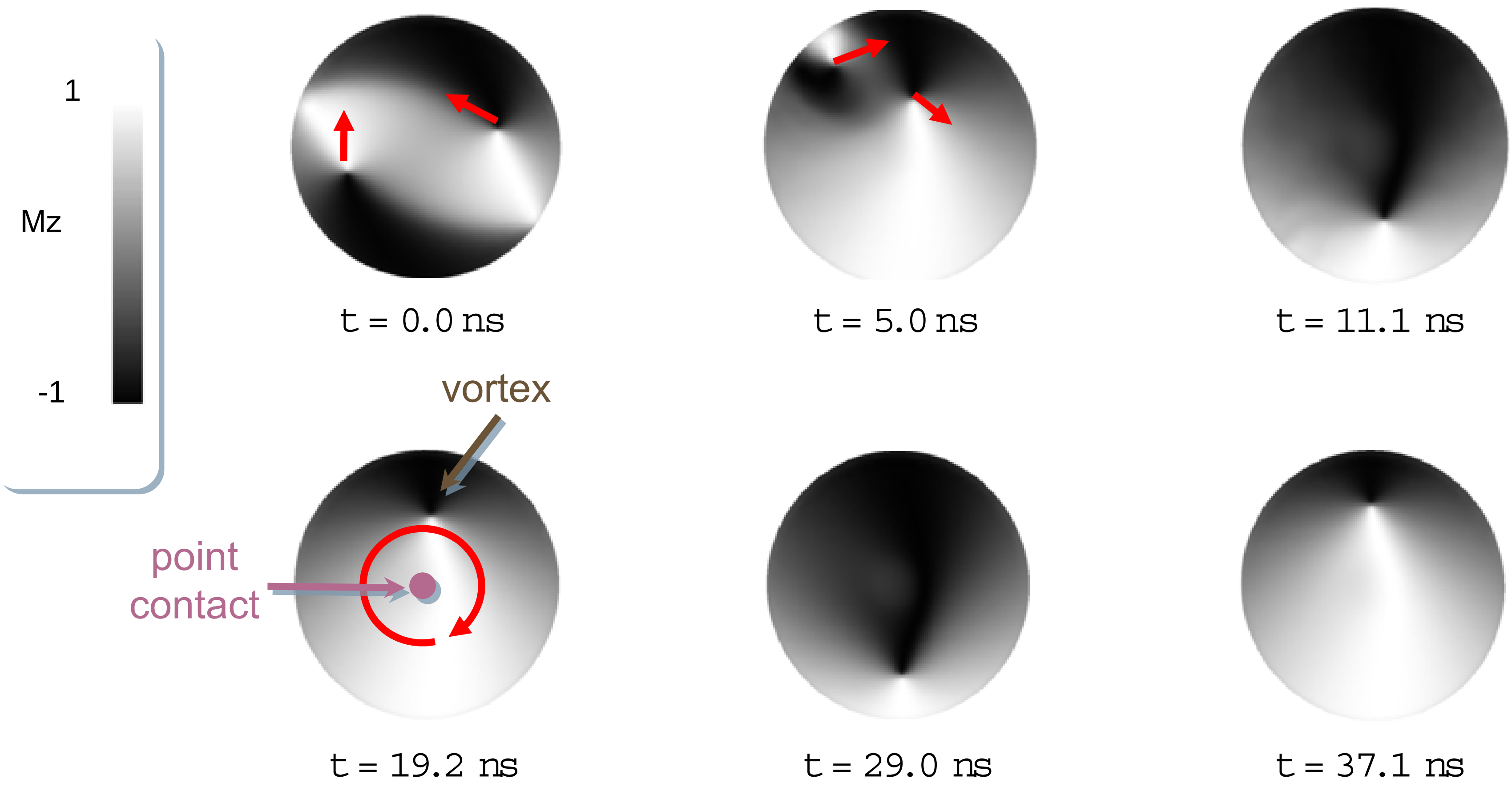

Comparison between simulation and experiment

Mistral, van Kampen, Hrkac et al., PRL **100**, 257201 (2008)

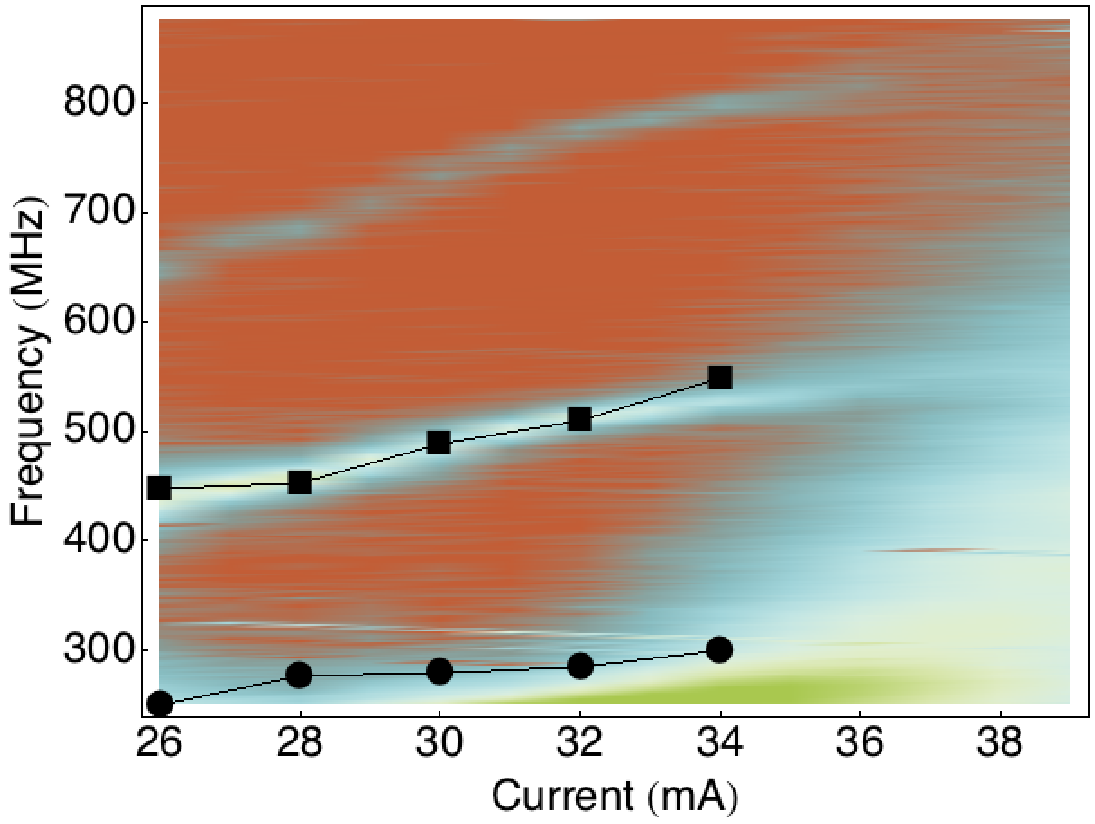

***H*perp = 3.5 kOe**

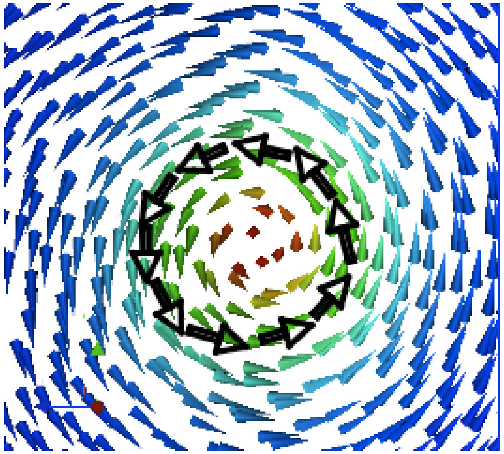

- **excellent agreement theory-experiment**
- **harmonics due to slightly elliptic trajectory (H_K)**

Rigid vortex model

Mistral, van Kampen, Hrkac et al., PRL **100**, 257201 (2008)

Seek to explain general trends with analytical model

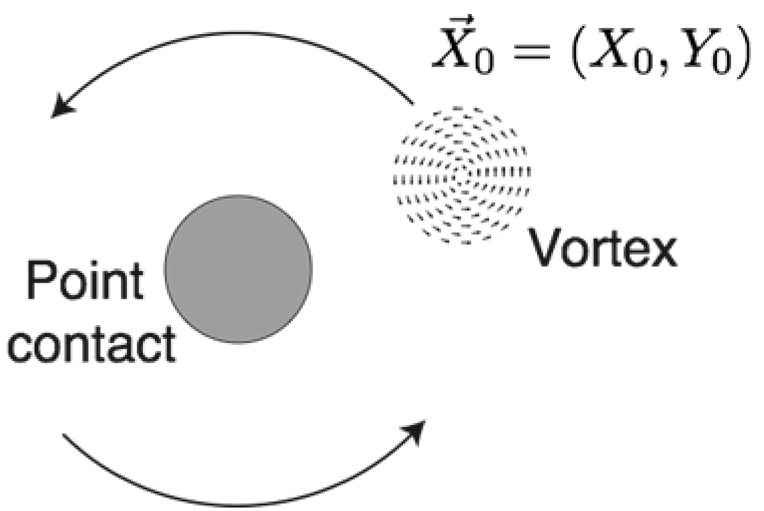

- Treat vortex as ***rigid object***
- Derive equations of motion with spin-transfer torque

Thiele equation + Slonczewski term

$$\vec{G} \times \frac{d\vec{X}_0}{dt} - \alpha \mathbf{D} \cdot \frac{d\vec{X}_0}{dt} + \sigma I \left(\vec{P}_\perp - \vec{P}_{||} \right) = \frac{\gamma}{M_s} \frac{\partial W}{\partial \vec{X}_0}$$

gryoscopic motion — damping — spin-transfer — force

Rigid vortex model

Mistral, van Kampen, Hrkac et al., PRL **100**, 257201 (2008)

Assume vortex is sufficiently far from contact region

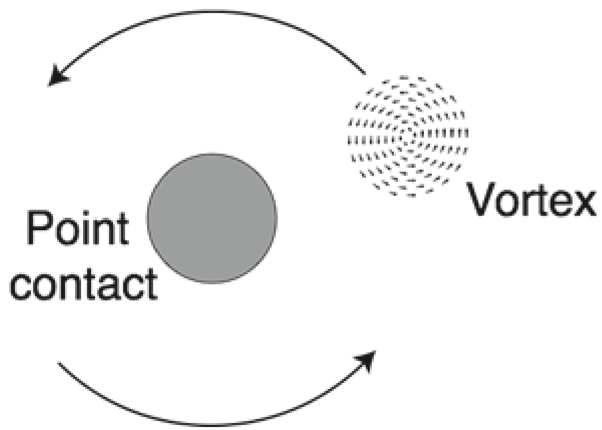

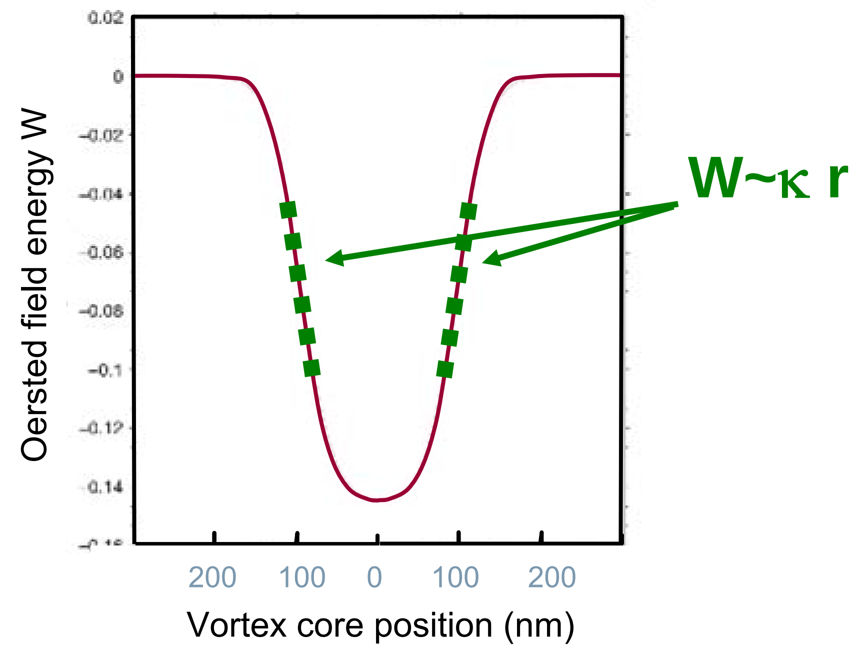

cf **motion in central potential**

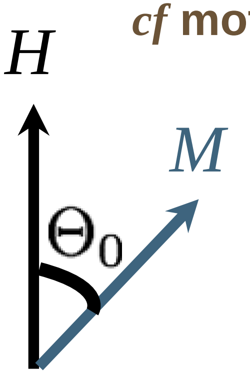

$$\omega = \left(\frac{1}{\pi a^2 d}\frac{\alpha D\kappa^2}{\sigma p_\perp}\right)\left(\frac{\gamma}{GM_s}\right)^2 \frac{I}{\sin^2\Theta_0}$$

Comparison between theory and experiment

Mistral, van Kampen, Hrkac et al., PRL **100**, 257201 (2008)

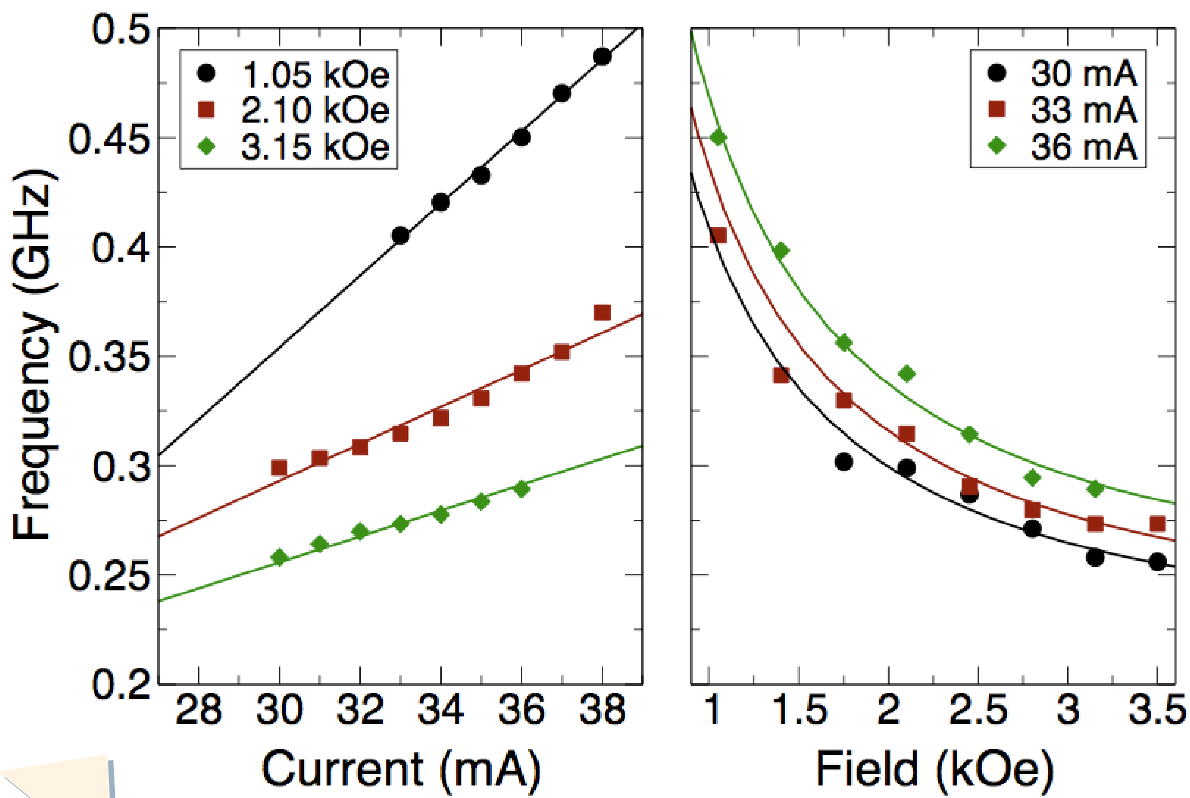

$$\omega \propto I$$

$$\omega \propto \left(\frac{H}{M_2} \left[1 - \left(\frac{H}{M_1} \right)^2 \right] \right)^{-1}$$

Summary: vortex oscillations

- Solid experimental evidence of current-driven vortex oscillations in metallic point-contacts
- < 500 MHz oscillations, tunable with current and perpendicular fields
- Good agreement with simulation and theory

• BLS studies on in nanopoint contacts

– Fabrication: IMEC

– Characterization: TUKL

Brillouin light scattering (BLS) process

= inelastic scattering of photons from spin waves

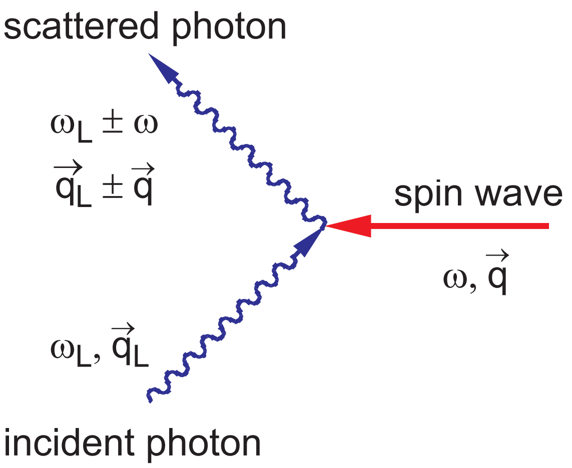

$$\vec{q}_{SC} = \vec{q}_L \pm \vec{q}$$

$$\omega_{sc} = \omega_L \pm \omega$$

spectrum of scattered light

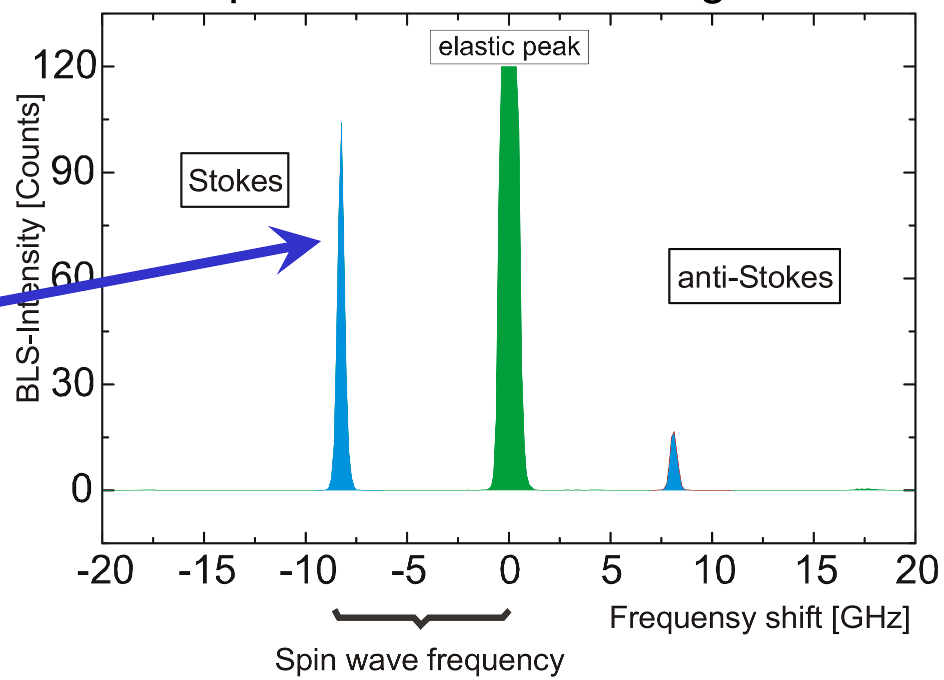

proportional to the
spin wave intensity $|\varphi|^2$

Point contact device geometries

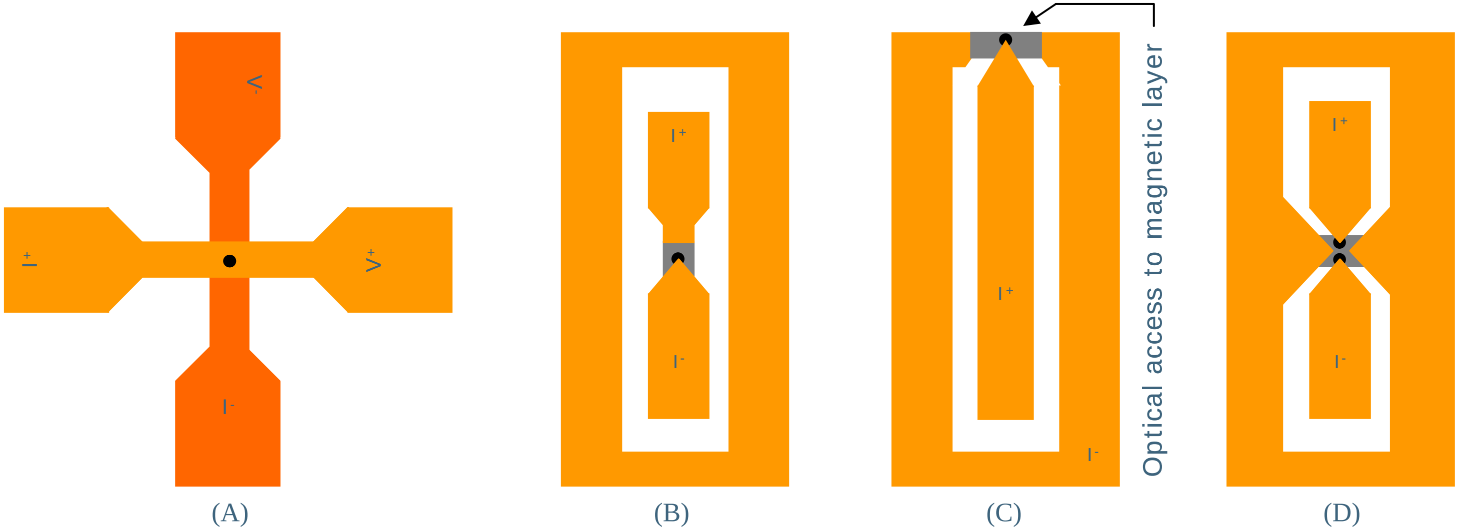

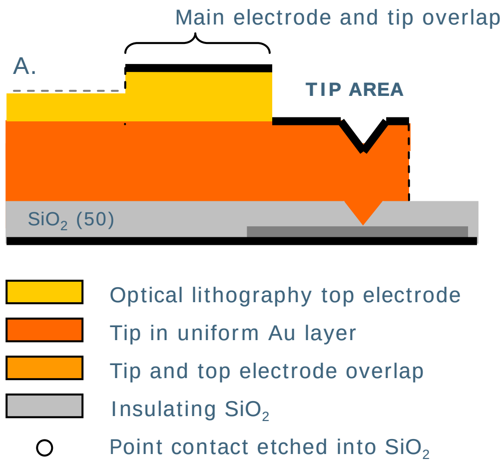

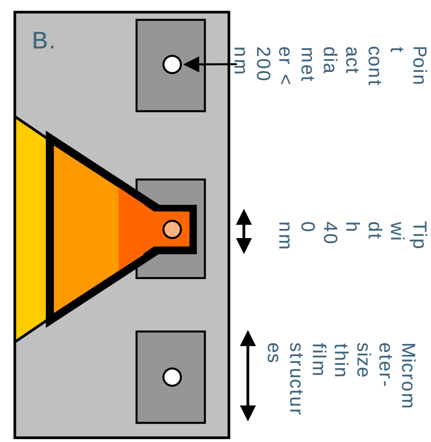

Device Fabrication

- Tip and top electrode overlap
- Au/Ti top electrodes
- Uniform Ti/Au layer
- Insulating SiO_2
- Thin film multilayer
- GaAs substrate
- Point contact etched into SiO_2

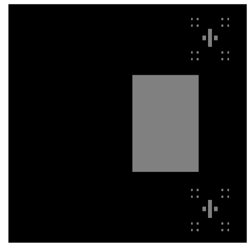

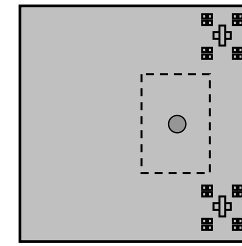

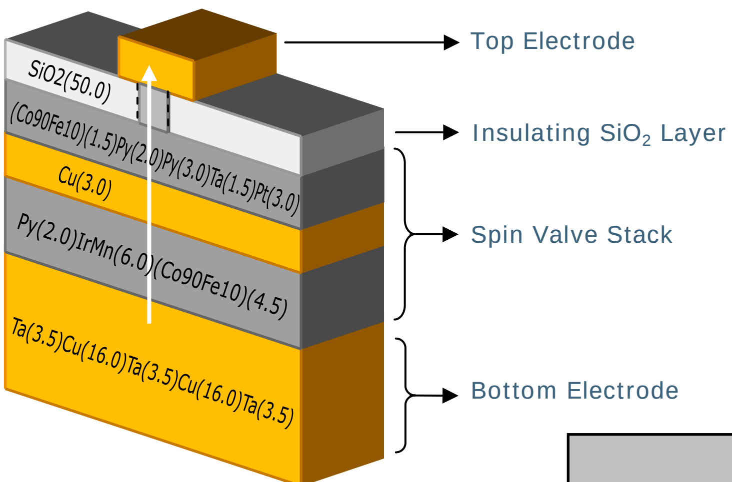

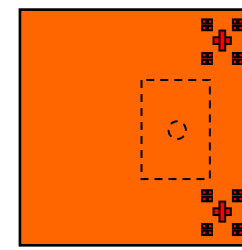

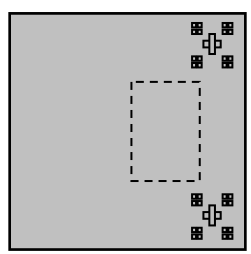

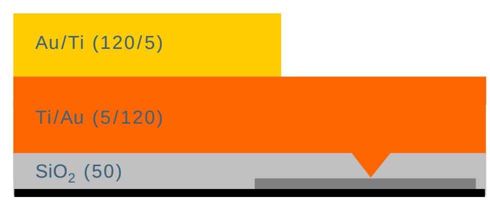

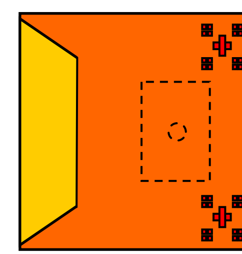

Device Fabrication

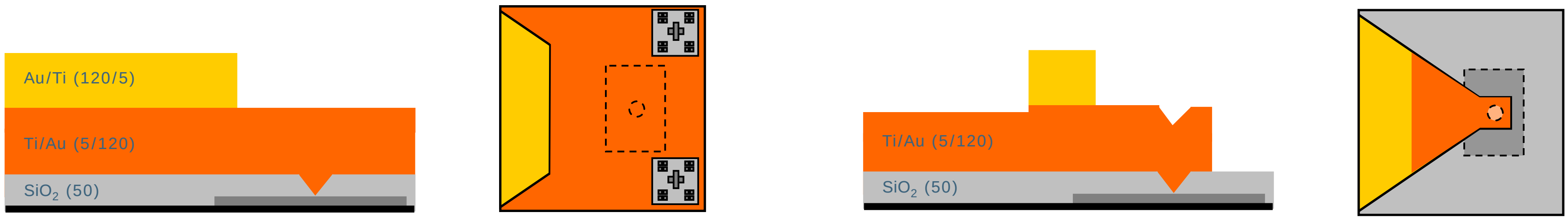

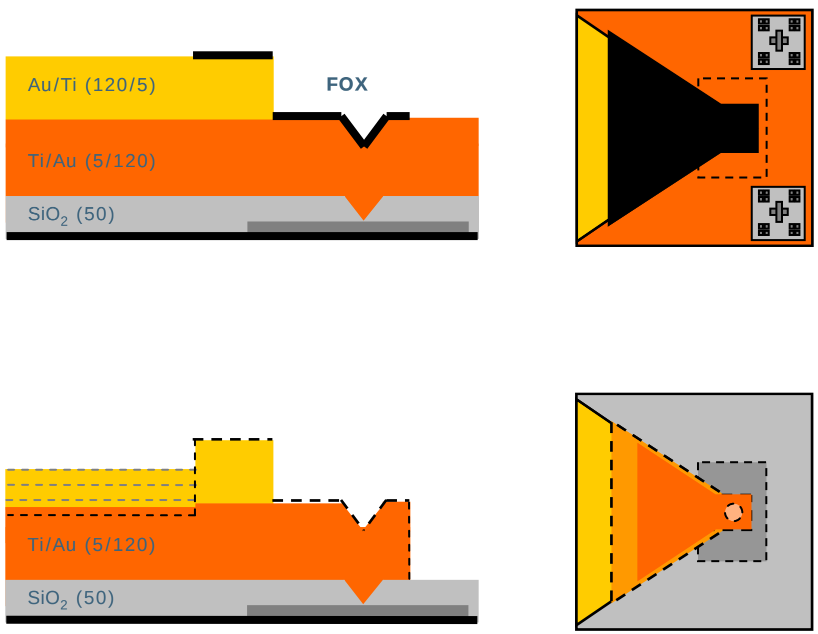

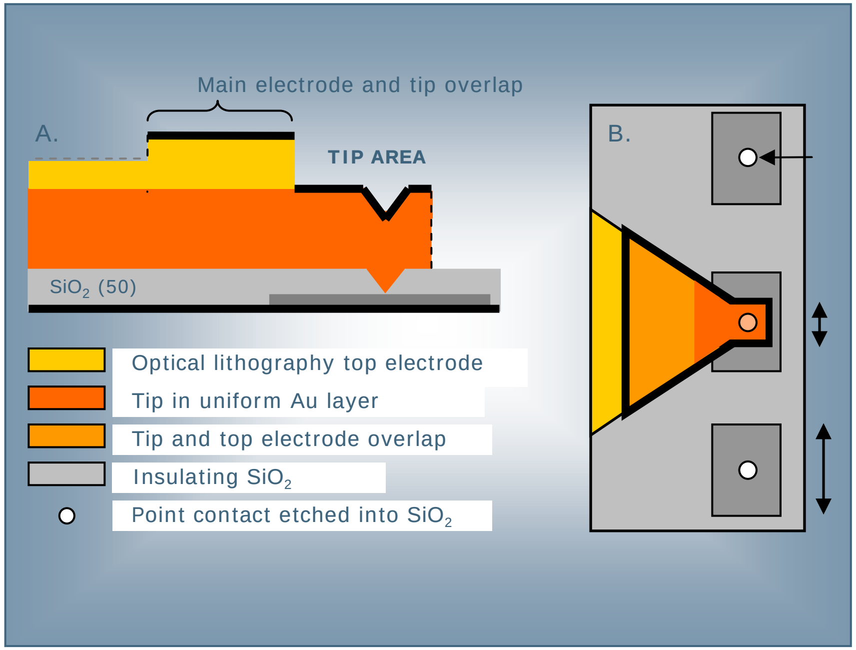

E.g. BLS device

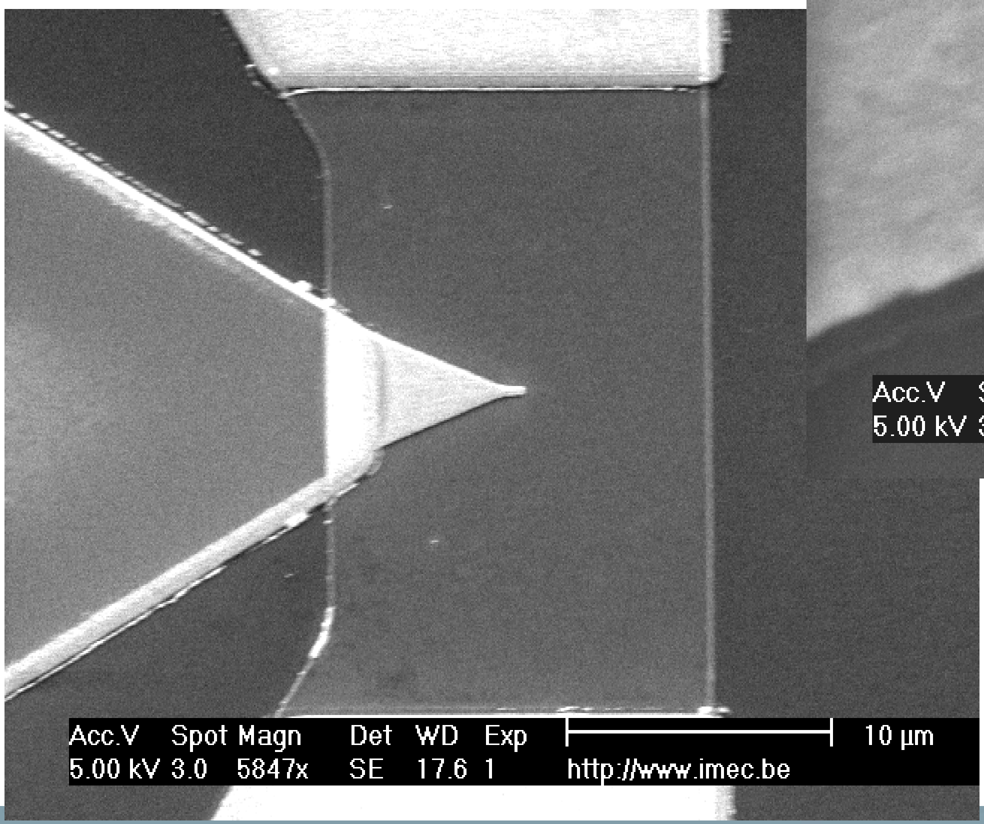

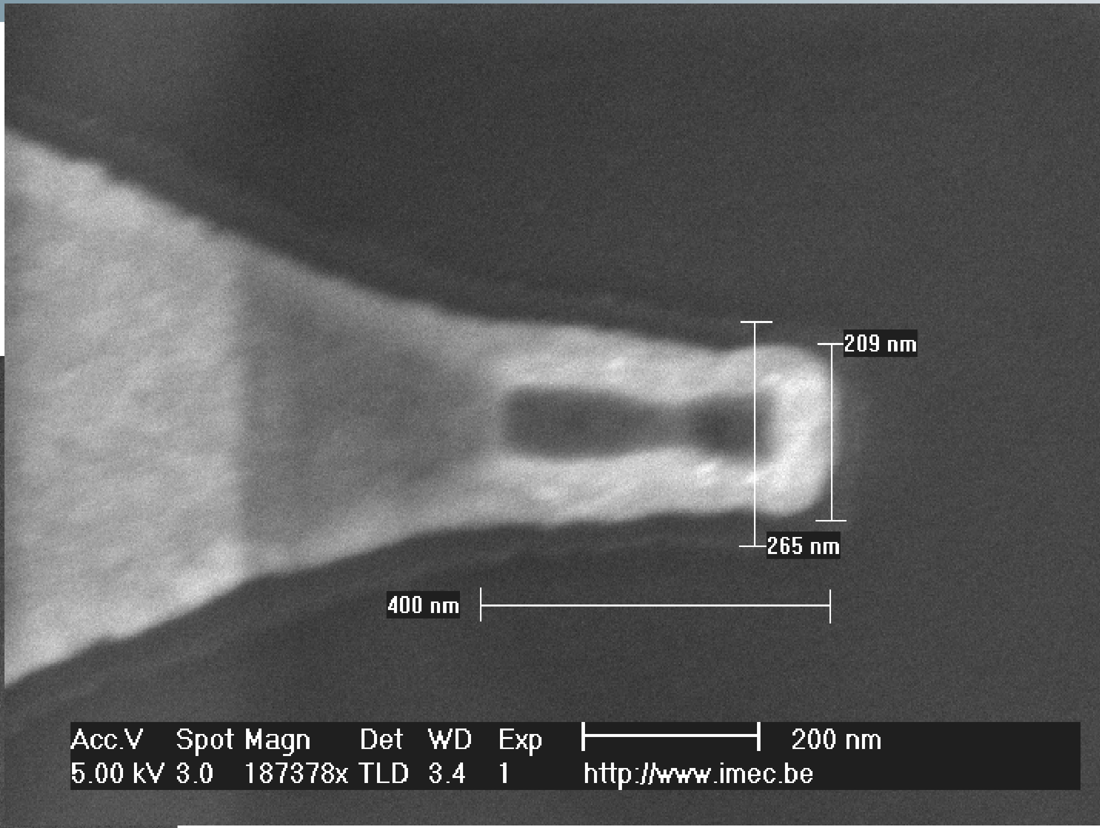

Brillouin Light Scattering Devices: Tip Breakdown

- Tip breakdown for high currents (>30 mA)

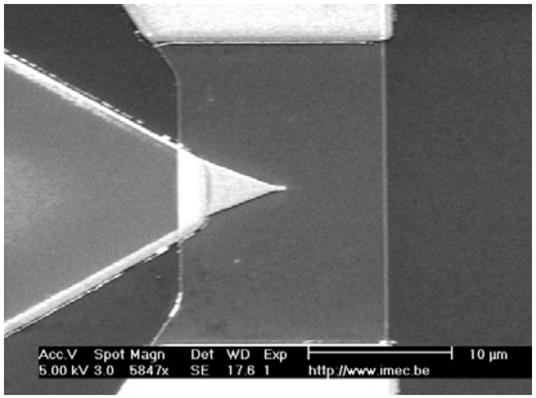

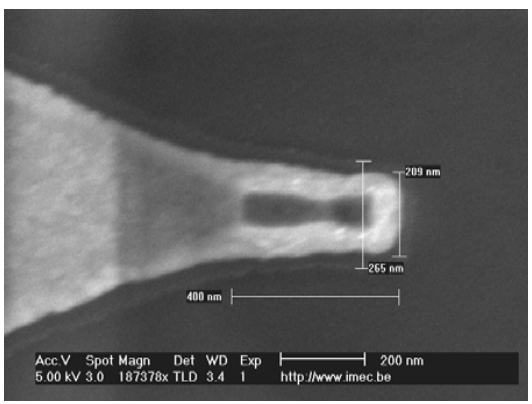

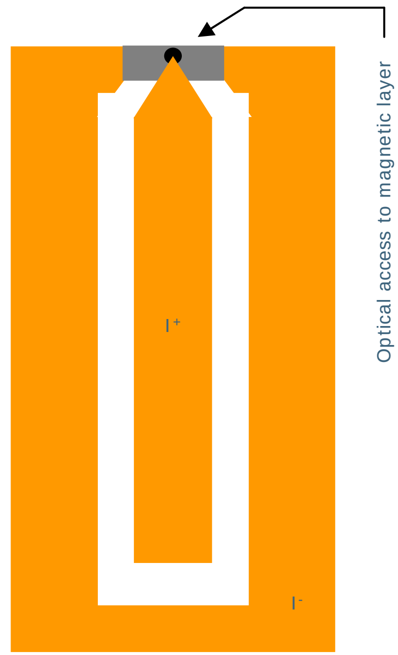

(C)

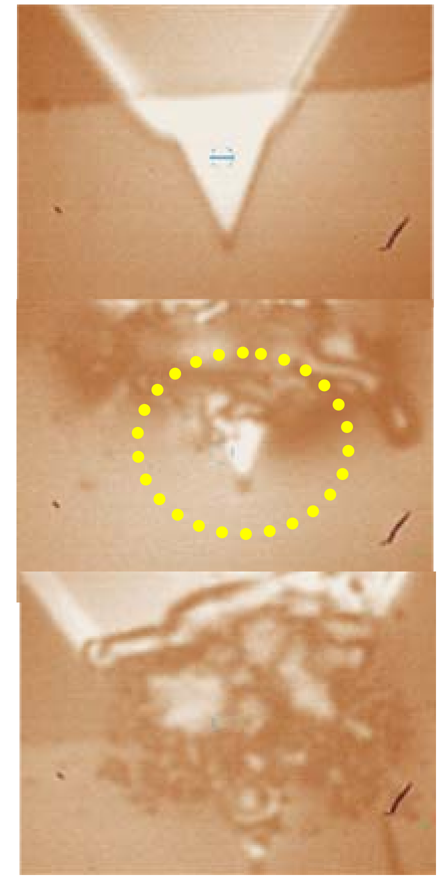

⇒ Mechanism? (Does the actual point contact survive?)

Radiation pattern of resonances

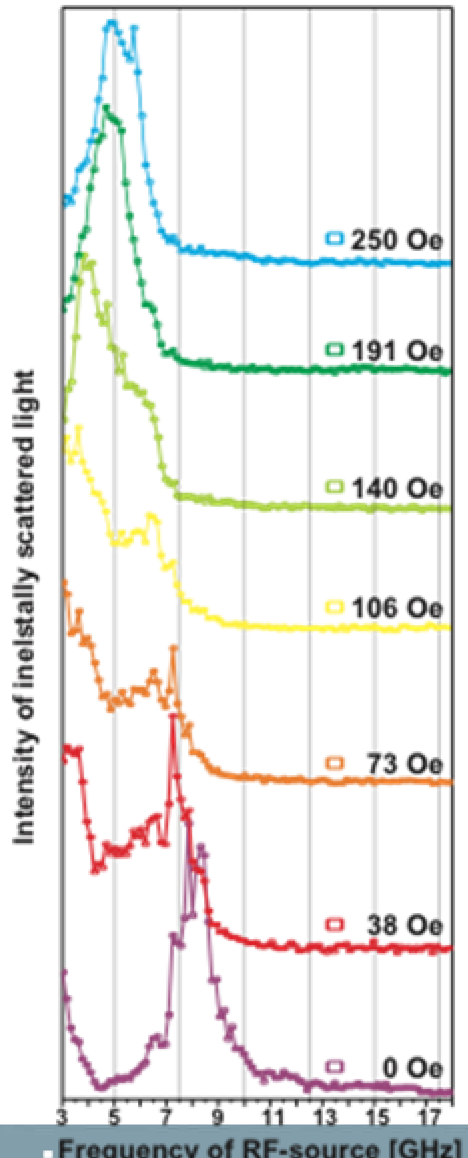

Characterization of dynamic properties: FMR with BLS-sensor

- constant position
- sweeping AC frequency for different magnetic fields

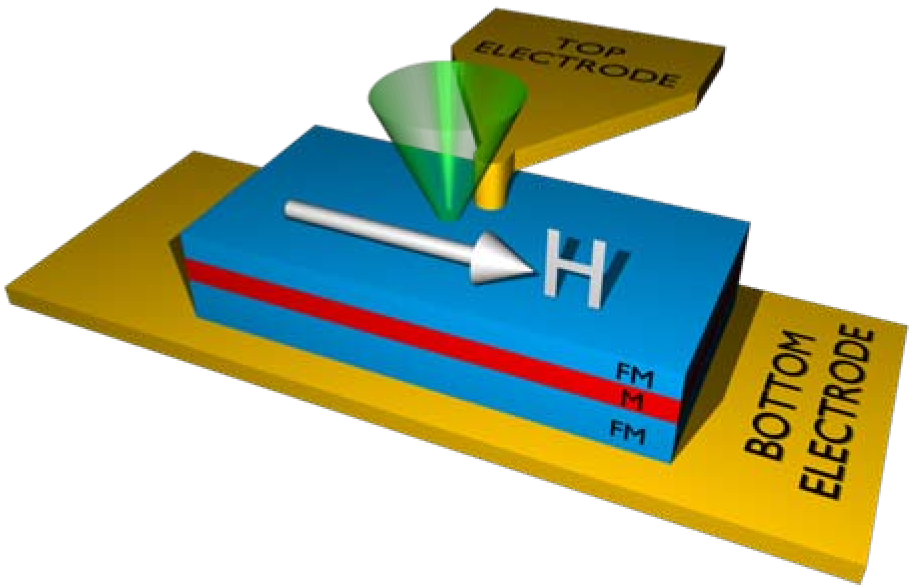

Radiation pattern of resonances

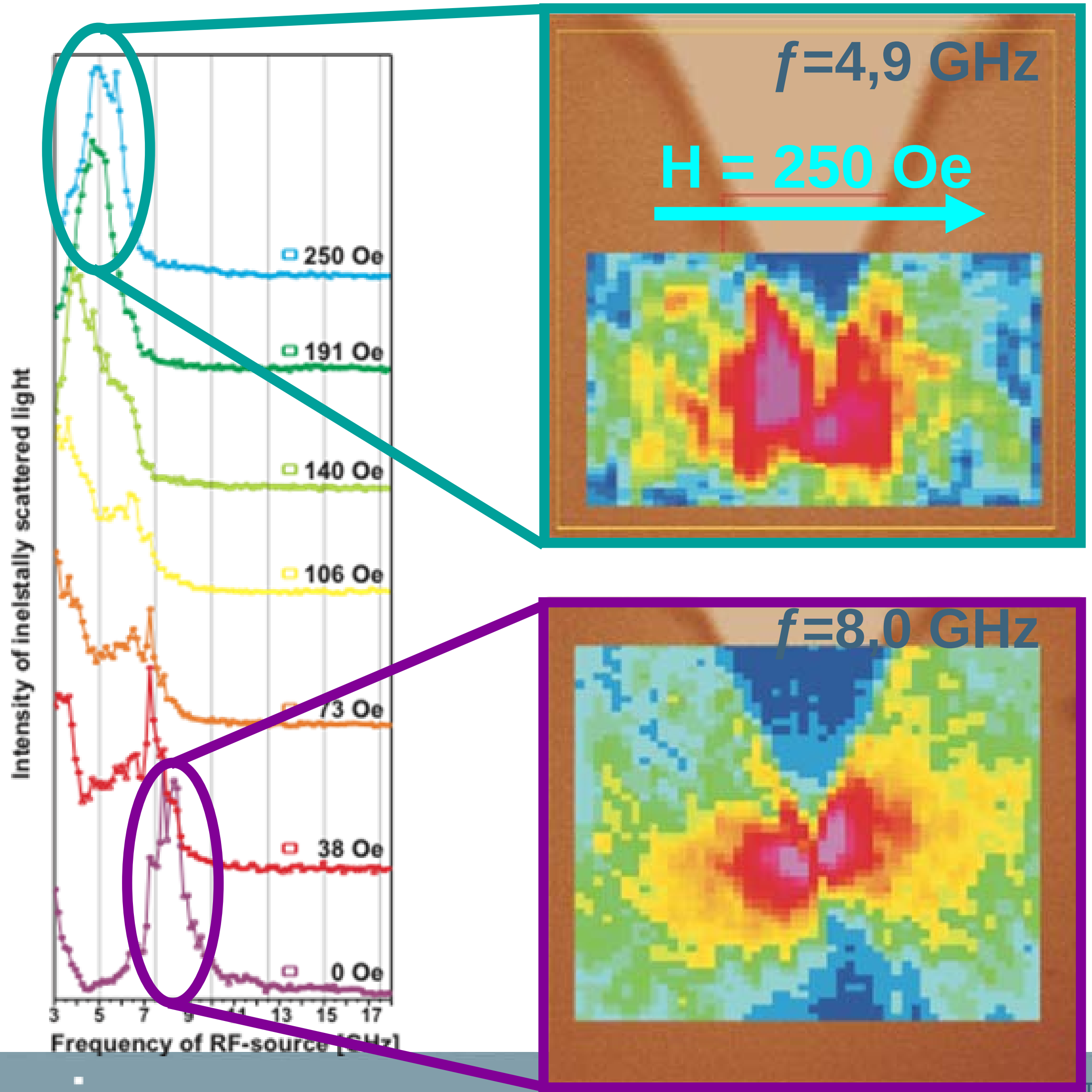

1 μm

- symmetric radiation around the nano-contact

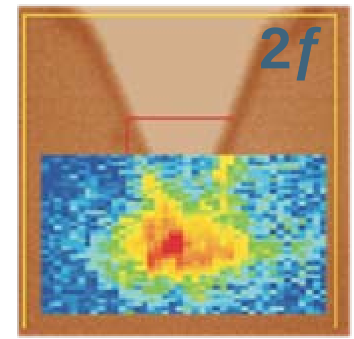

- asymmetric radiation in horizontal direction

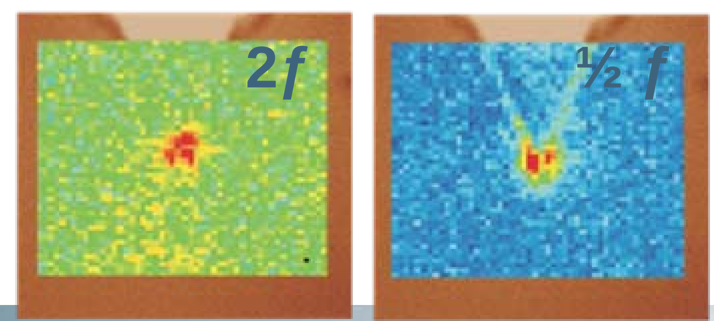

Nonlinear phenomena

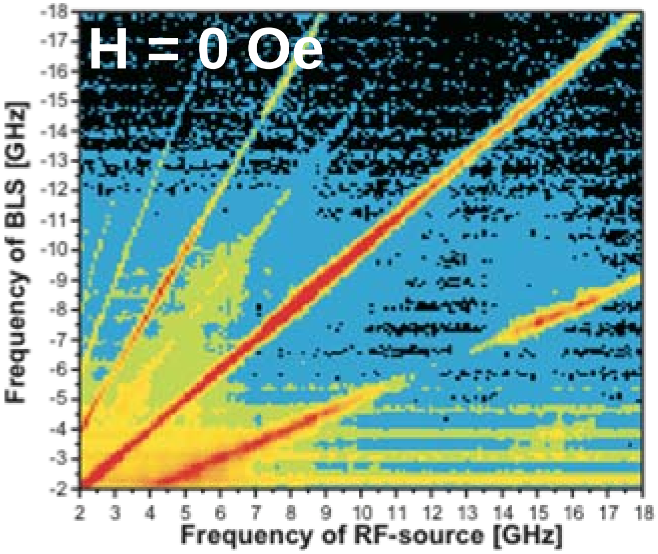

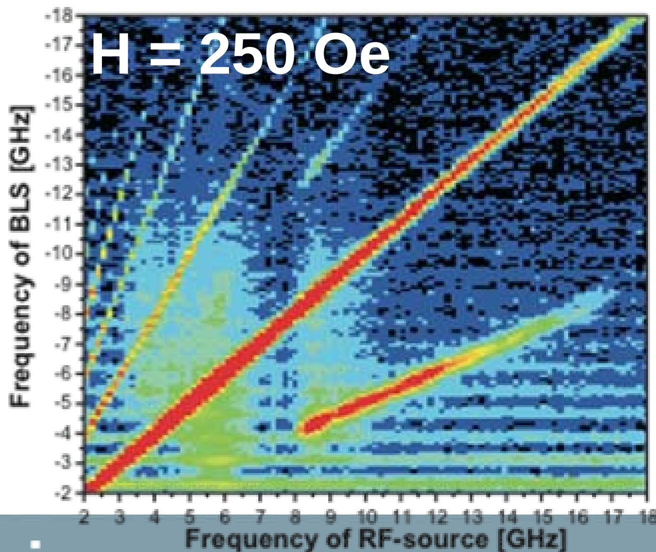

- Constant position close to the point contact
- Sweeping the externally applied ac-frequency

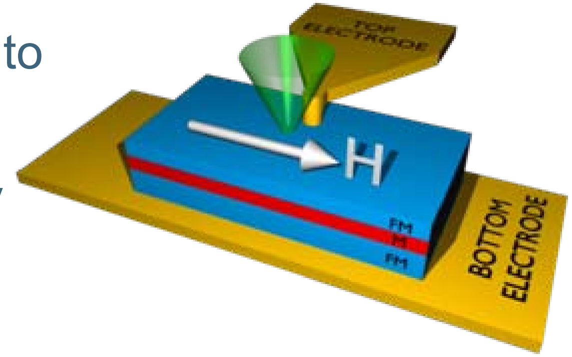

➡ **Higher frequency generation**
2*f*, 3*f*, 4*f*

➡ **Half frequency generation**
½ *f*, 1½ *f*

3 magnon processes

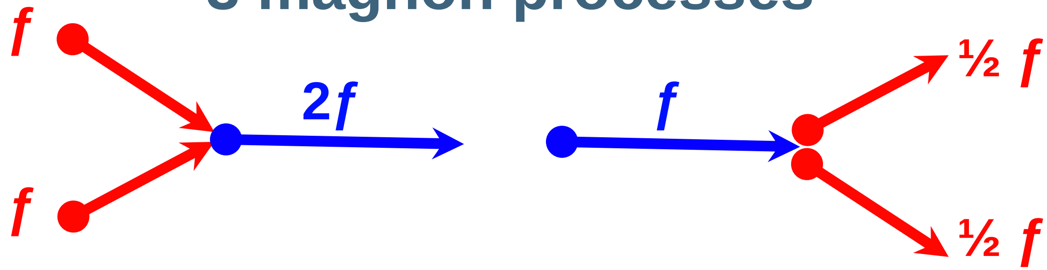

Nonlinear phenomena

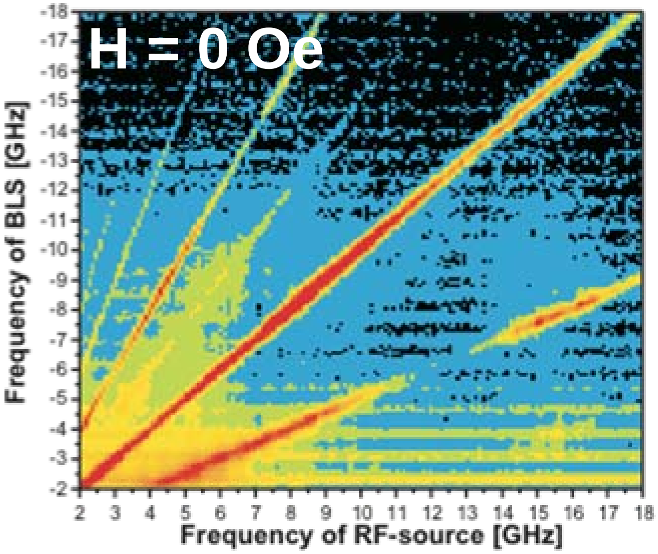

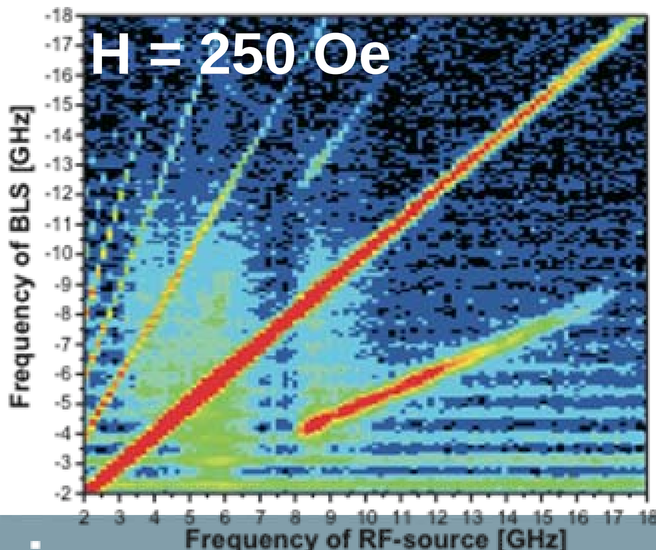

Conservation of energy and momentum in 3 magnon processes:

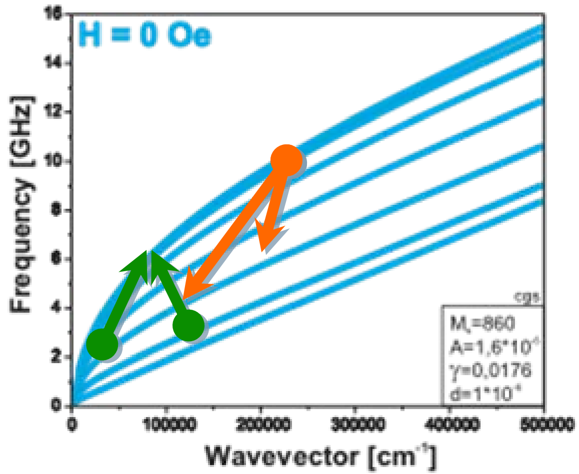

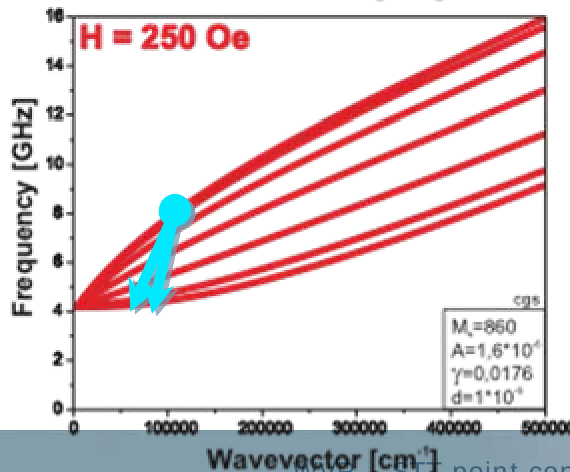

- ½*f* generation only if pumping frequency is at least twice the bottom of the spin wave band

imec

Nonlinear phenomena and DC current induced effects

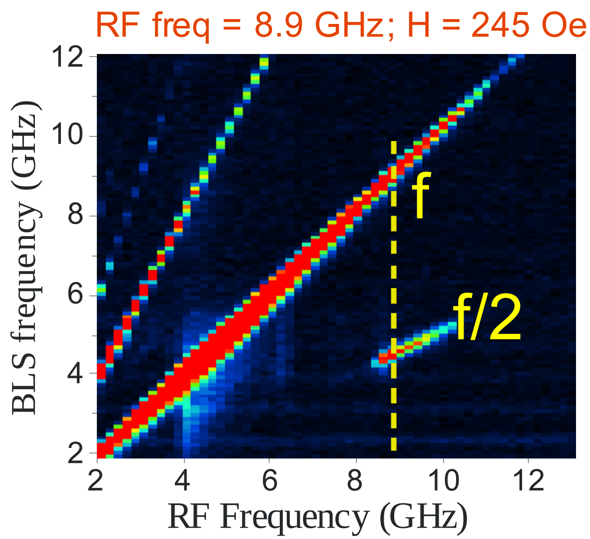

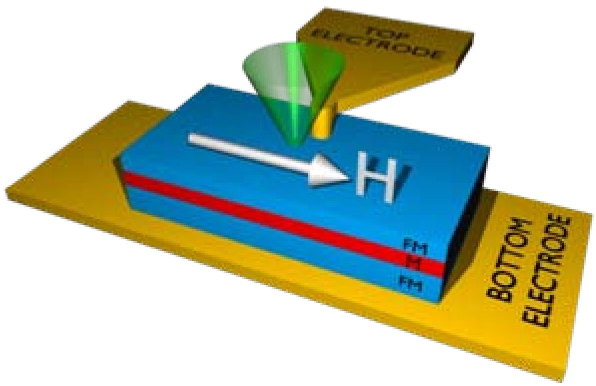

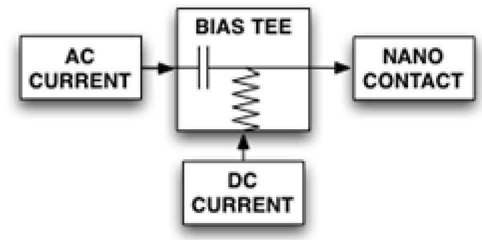

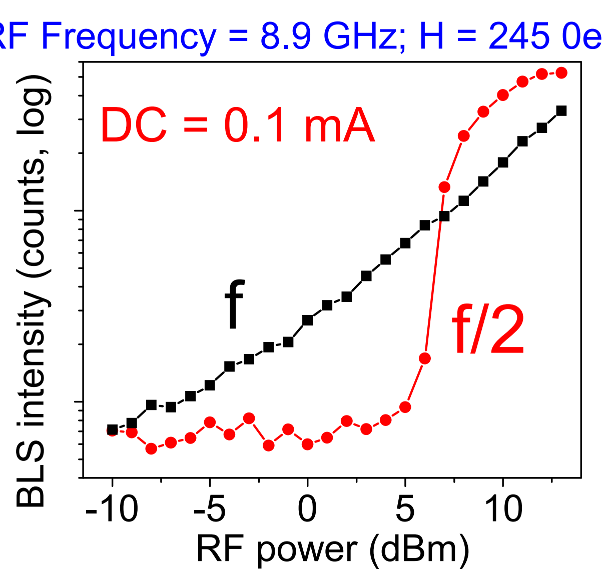

- Investigation of the power threshold for nonlinear frequency conversion as function of the DC current

The Resonance mode increases linearly with the applied RF-power
- ½*f* shows clearly threshold behavior

Threshold properties depends on internal losses (damping)

DC current induced effects

Threshold power (for half mode generation) dependence as function of the DC current for H = 245 0e and RF freq = 8.9 GHz

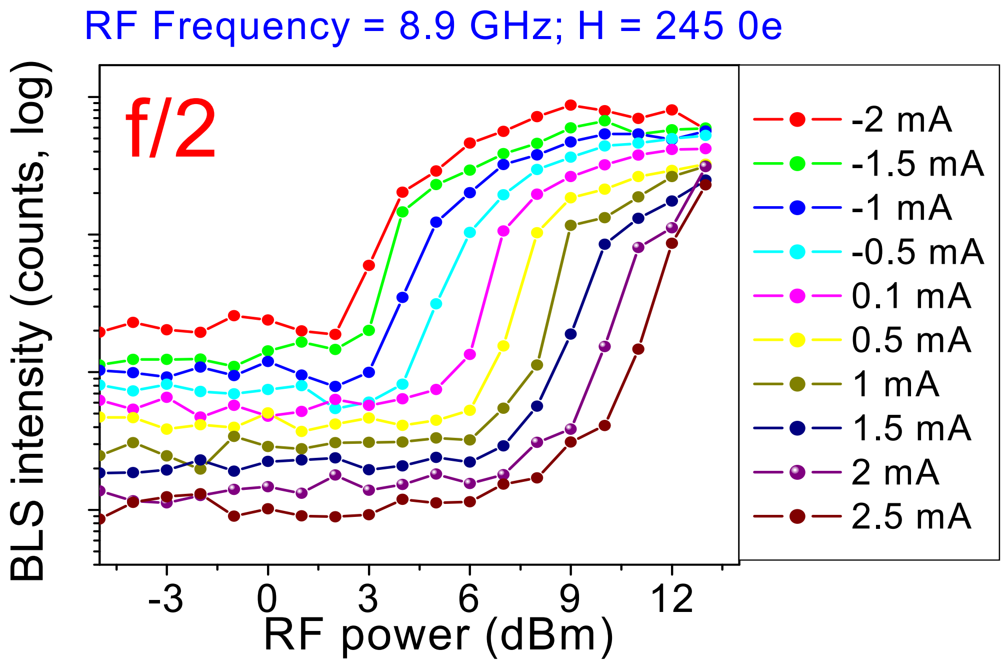

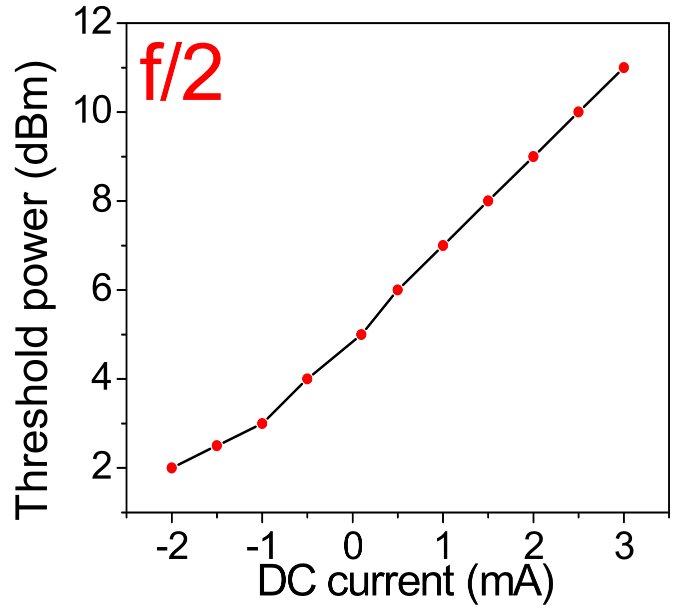

- Shift of the power threshold for the 3-magnon scattering probability
- Control of the effective damping due to DC-current: Spin torque effect!

DC current induced effects

Measure the threshold power dependence as function of the DC current and the X scan position from the point contact

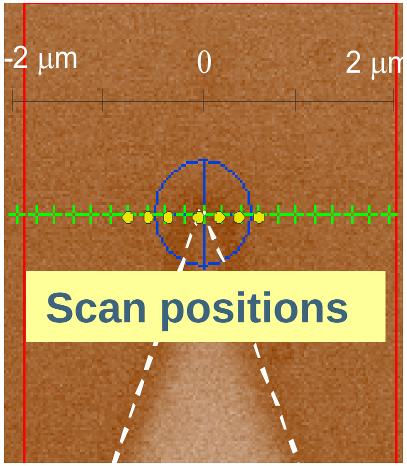

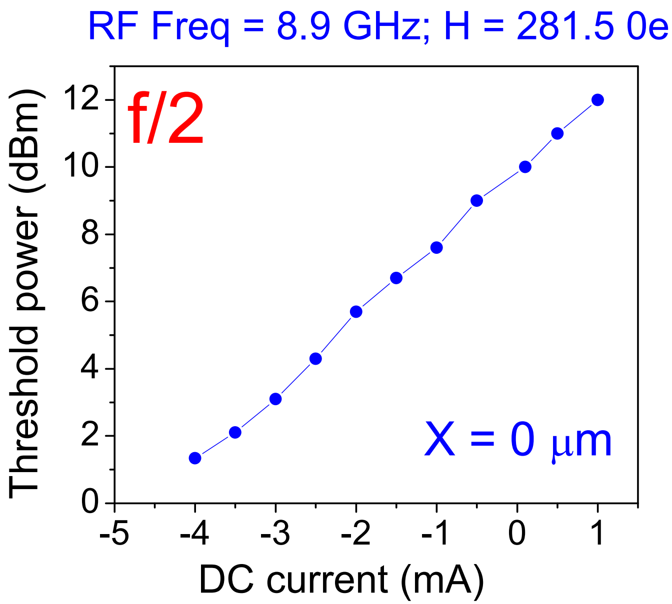

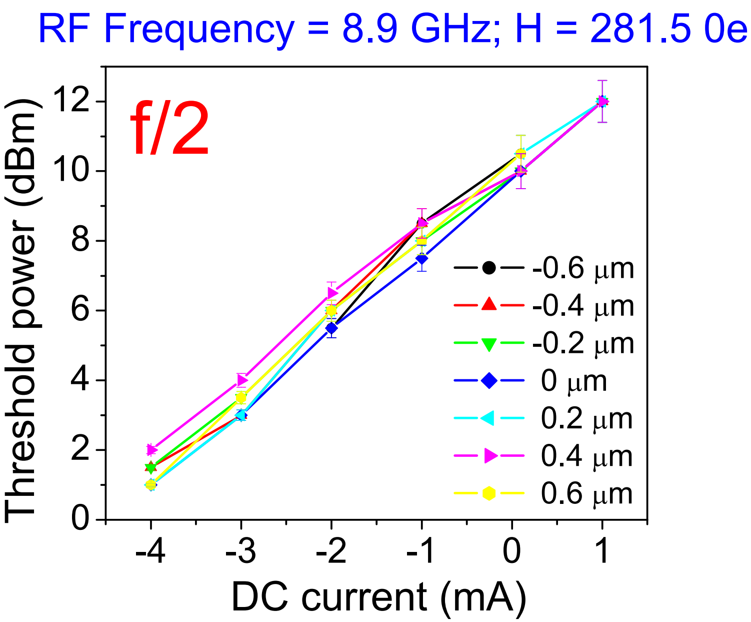

No effect of the scan position on the dependence of the shift of the power threshold for the 3-magnon scattering probability as function of the dc current: Spin torque effect and no effect of the Oersted field (= spatial dependence) ?

DC current induced effects

Measure the threshold frequency for half frequency generation as function of the DC current and the scan position from the point contact:
Know the effect of the spin torque effect or the Oersted field on the shift of dispersion curves

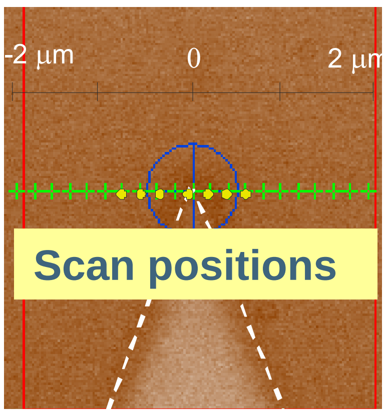

H = 281.5 0e, X = 0 µm; DC = 0.1 mA

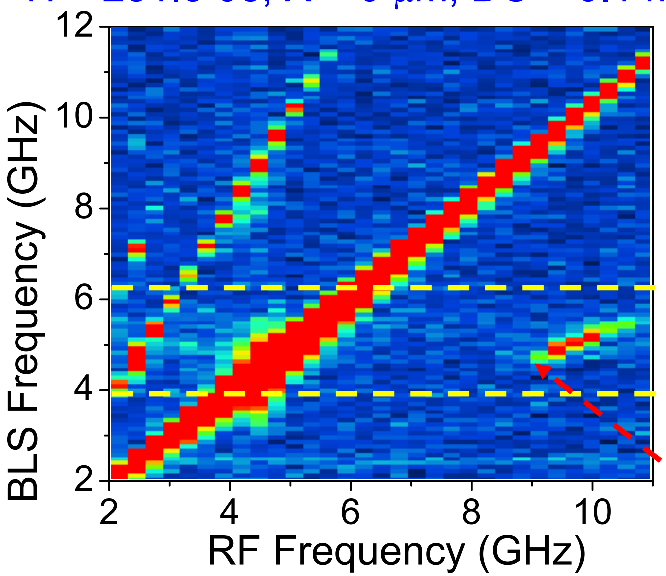

H = 281.5 Oe; x= 0 µm

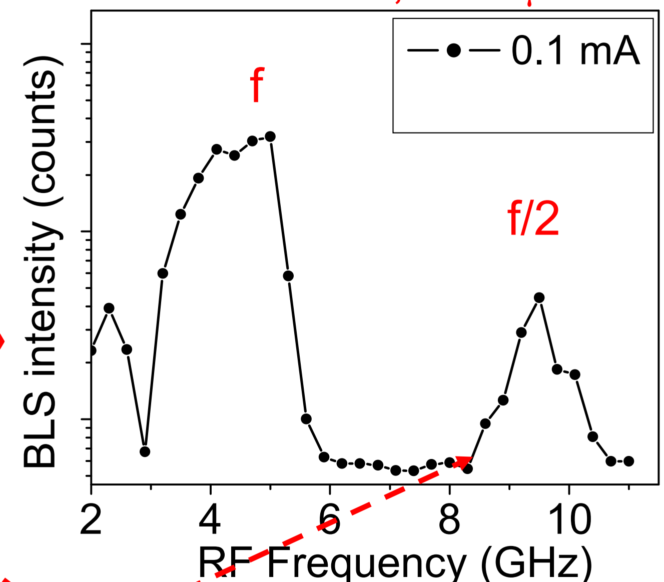

Threshold frequency

DC current induced effects

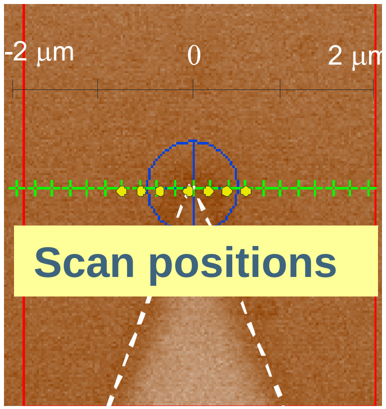

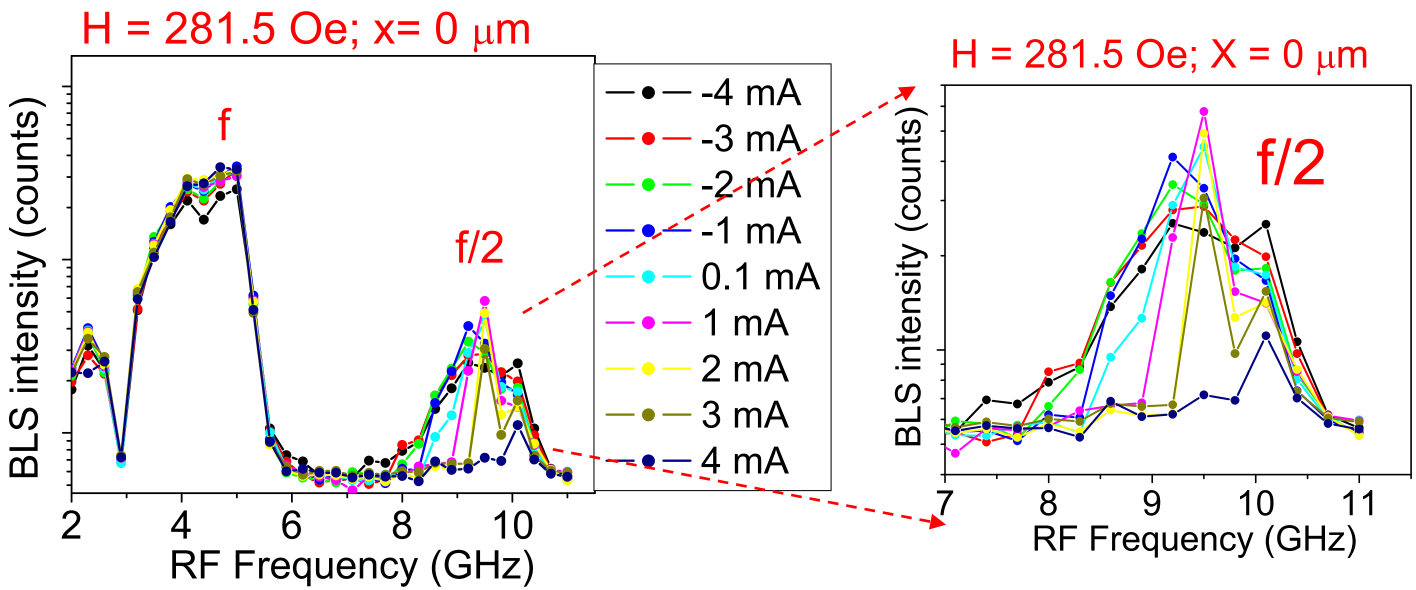

DC current induced a shift of the threshold frequency for f/2 mode generation: Spin torque effect or Oersted field effect?

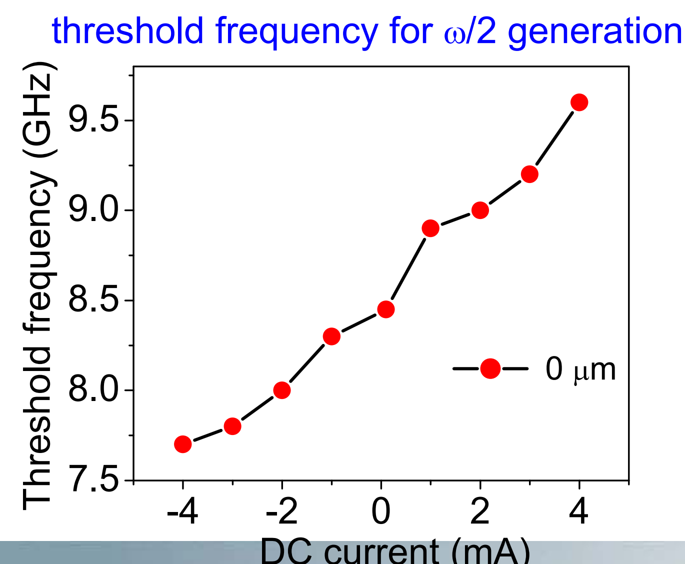

DC current induced effects

Measure the threshold frequency for half frequency generation as function of the DC current and the scan position from the point contact:

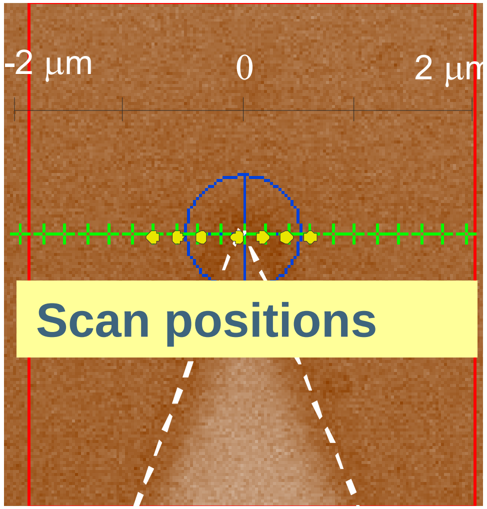

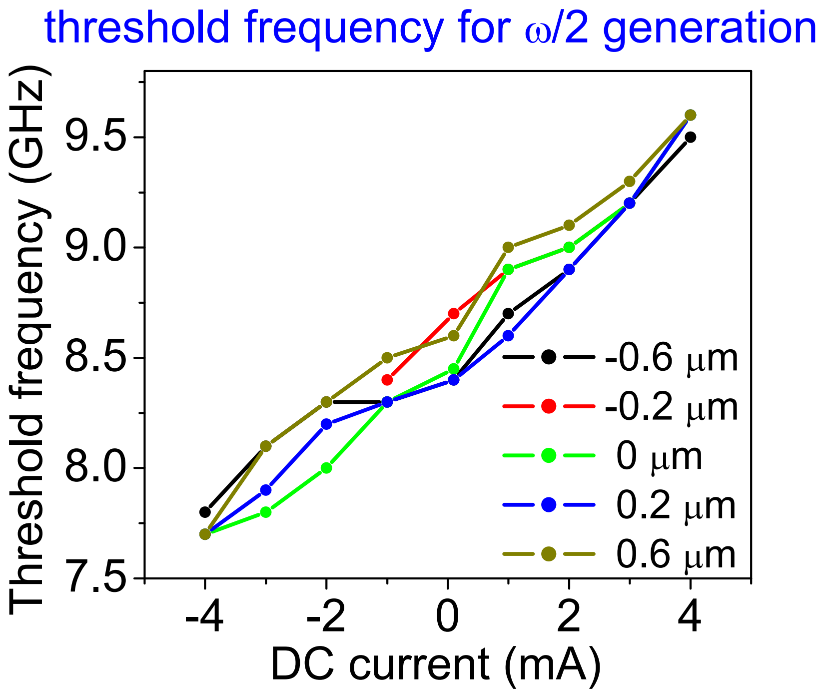

- ❑ DC current induced a shift of the threshold frequency for f/2 generation
- ❑ No effect of the X scan position (left and right from the point contact) on the threshold frequency dependence as function of the DC current : Spin torque effect and not Oersted field effect! (Oersted field effect = spatial dependence with distance from the point contact)!

Conclusion and perspectives

- Conclusions:
  - Dc current induced a shift of the power threshold for the 3-magnon scattering probability and the threshold frequency for half frequency mode generation
  - control of the effective damping due to DC-current
  - No effect of the scan position on the dependence of the threshold properties of 3-magnon scattering decay (power and frequency) as function of the dc current

  $\Rightarrow$ Spin torque effect and no effect of the Oersted field?

- Perspectives:
  - Understand more the effect of spin torque transfer in nonlinear spin dynamics system

aspire invent achieve